The effect of monosaccharide reducing sugars on the atom transfer radical polymerization of n-butyl methacrylate and methyl methacrylate

by

A.R. De Vries

Thesis presented for the degree

Master of Science (Polymer Science)

at the

University of Stellenbosch

Promoter: **Prof. B. Klumperman**
Technological University of Eindhoven

Co-promoters: **Prof. R.D. Sanderson**
University of Stellenbosch
Dr. D. de Wet-Roos
Plascon Research Centre

External Examiner: **Prof. G.J. Summers**
University of South Africa

December 2001

DECLARATION

I, the undersigned hereby declare that the work contained in this thesis is my own original work and has not previously in its entirety or in part been submitted at any university for a degree.

Andrew De Vries

Date

March 30, 2001

_____

SUMMARY

The effect of various organic reducing agents, in the form of monosaccharide reducing sugars, on the rate of atom transfer radical polymerization (ATRP) of n-butyl methacrylate and methyl methacrylate is reported in this study. The addition of the reducing sugars has a positive effect on the rate of ATRP. Up to 100% increase in the rate of polymerization was recorded, in some cases. These organic reducing agents have little effect on the molecular weight and molecular weight distribution of the poly(n-butyl methacrylate) and polydispersity indexes remain well below 1.2. The molecular weight of the poly(methyl methacrylate), when glucose and galactose are added to the reaction mixture, compares well with the theoretical expected values.

An explanation for these observations is the ability of the reducing sugars to reduce part of the Cu(II) species, that serves to deactivate the growing radicals, to Cu(I), thereby ensuring a shift in the equilibrium between active and dormant chains in the direction of the former and a resulting increase in the rate of polymerization.

UV/VIS spectroscopy and cyclic voltammetry were used to investigate the mechanism behind the polymerization rate enhancement.

OPSOMMING

In hierdie studie word die effek van verskeie organiese reduseermiddels, in die vorm van monosakkaried reduserende suikers, op die tempo van polimerisasie van ATRP gerapporteer. Hierdie reduserende suikers het 'n positiewe effek op die polimerisasie tempo. In sommige gevalle word 'n toename van 100% in die polimerisasie tempo waargeneem. Die organiese reduseermiddels het 'n minimale effek op die molekulere massa en molekulere massa verspreiding (in meeste gevalle minder as 1.2) van die poly(n-butiel metakrielaat). In die geval van die poly(metiel metakrielaat), wanneer glukose en galaktose by die reaksie mengsel gevoeg word, stem die molekulere massas goed ooreen met die teoreties voorspelde molekulere massas.

Die waargenome toename in die polimerisasie tempo kan toegeskryf word aan die vermoe van die reduserende suikers om die Cu(II), wat dien om die groeiende radikale te deaktiveer, gedeeltelik te reduseer na Cu(I). Hierdeur word verseker dat die ewewig tussen die aktiewe en dormante kettings in die rigting van die eersgenoemde verskuif word, wat dus aanleiding gee tot 'n toename in die polimerisasie tempo.

Ultraviolet spektroskopie en sikliese voltammetrie is ook gebruik om lig te werp op die meganisme agter die toename in die tempo van polimerisasie.

DEDICATION

I hereby dedicate this thesis to everyone who ever influenced my life in a positive way. I also dedicate this work in loving memory of my father, Stanley, and my brother, Richard.

CONTENTS

LIST OF FIGURES

LIST OF TABLES AND SCHEMES

LIST OF TABLES

LIST OF SCHEMES

LIST OF ABBREVIATIONS

ATRA: Atom transfer radical addition

ATRP: Atom transfer radical polymerization

AIBN: Azoisobutyronitrile

Br: Bromide

Cl: Chloride

Cu: Copper

i: Current

CV: Cyclic voltammetry

GC: Gas chromatography

GPC: Gel permeation chromatography

$[M]_0$: Initial monomer concentration

I: Initiator

Fe: Iron

MMA: Methyl methacrylate

M: Monomer

n-BMA: n-Butyl methacrylate

M_n: Number-average molecular weight

R-X: Organic halide

PMDETA: Pentamethyldiethylenetriamine

E: Potential

k_a: Rate constant of activation

k_d: Rate constant of deactivation

k_t: Rate constant of termination

$[M]_t$: Residual monomer concentration

TsCl: Toluene-4-sulfonyl chloride (Tosyl chloride)

M_t^{n+1}: Transition metal species in higher oxidation state

M_t^n: Transition metal species in lower oxidation state

UV/VIS: Ultra violet/visible

$\mathbf{M_w}$: Weight-average molecular weight

ACKNOWLEDGEMENTS

I wish to express my sincere thanks to:

Prof. R.D. Sanderson, Director of the UNESCO Macromolecular Centre, University of Stellenbosch, for his support and encouragement.

Dr. D. De Wet-Roos, Senior Researcher, Plascon Ltd., for all his guidance and assistance. Thank you for always being willing to help me.

Prof. B. Klumperman, Technical University of Eindhoven, The Netherlands, for his advice.

Prof. A.M. Crouch, Dept. of Chemistry, for all his help with the cyclic voltammetry.

Margie Hurndall, for taking such care in sorting out the grammar and for her suggestions. Thanks for all your time and effort.

My mother, Lettie, for all her sacrifices over the years.

My brothers and sisters, you know who you are, for investing in my life.

Llewellyn Davids, a true friend, for all his assistance. Thanks for always being willing to go the extra mile for me.

Thanks be to God who always causes me to triumph.

(All glory belongs to You, Lord!)

1. INTRODUCTION AND OBJECTIVES

1.1 Introduction

Conventional free radical polymerization is one of the most important processes for the synthesis of high molecular weight polymers. A major advantage of conventional free radical polymerization is the fact that a wide variety of monomers can be successfully polymerized and copolymerized, under various conditions. Conventional free radical polymerization is not as sensitive to impurities as its ionic polymerization counterparts are. Conventional free radical polymerization does, however, have one major disadvantage; there is no control over molecular weights and polydispersities due to extensive chain termination and transfer reactions. This limitation of conventional free radical polymerization precludes the synthesis of well-defined polymers with controlled microstructure and morphology. Fortunately, conventional free radical polymerization can be controlled under conditions where a fast, dynamic equilibrium exists between dormant (non-radical) and active (radical) species and only a low, stationary concentration of the active species is maintained. The controlled or 'living' free radical polymerization processes that utilize the aforementioned principle are nitroxide- and cobalt- (only with acrylates) mediated controlled polymerization and reversible addition fragmentation chain-transfer (RAFT) polymerization. Atom transfer radical polymerization (ATRP) is also a member of the family of controlled free radical polymerization processes.

ATRP and nitroxide-mediated controlled radical polymerization rely on reversible activation of a dormant polymer chain. The only fate of the "counter-radical", halide or nitroxide, is to reversibly combine with the growing active chain. Upon bimolecular termination of growing polymer chains, an excess of the "counter-radical" will build up. This eventually leads to a shift in the equilibrium between active and dormant species and a decrease in the rate of polymerization. One way to overcome the above-mentioned reduction in polymerization rate, in the case of ATRP, is by using zerovalent metals (such as Cu^0) as inorganic reducing agents (for Cu^{2+}). The principle was shown to work in the ATRP of methyl acrylate, methyl methacrylate and styrene.[1] The abovementioned approach rests on the premise that the rate of polymerization is dependent on the Cu^{1+} / Cu^{2+} ratio (Equation 1.1).[2]

$$R_p = k_p K_{eq}[M][RX]_0 \frac{[Cu^{1+}]}{[Cu^{2+}]} \qquad (1.1)$$

where: R_p is the rate of polymerization;

k_p is the propagation rate constant of polymerization;

K_{eq} ($=k_a/k_d$) is the equilibrium constant;

k_a and k_d are the rate constants of activation and deactivation, respectively;

[M] is the monomer concentration;

$[Cu^{1+}]$ and $[Cu^{2+}]$ are the copper concentrations in the lower and higher oxidation states, respectively.

A possible disadvantage of the use of the zerovalent metal as a reducing agent, is the further increase in the (usually already large) copper concentration in the system due to the oxidation of Cu^0 to Cu^{1+}.

1.2 Objectives

In this study we investigated the use of organic reducing agents, in the form of monosaccharide reducing sugars, as a suitable alternative to Cu(0) as reducing agent for Cu(II) in the atom transfer radical polymerization of n-butyl methacrylate and methyl methacrylate. Enhancement of the polymerization rate, while still maintaining the necessary control over molecular weight and molecular weight distribution, was also investigated.

The idea of using monosaccharide reducing sugars to enhance the rate of polymerization rate stems from the use of sugars as reducing agents in redox initiated polymerization.[3] In that system, Fe^{2+} was used to activate a hydroperoxide where one oxygen-centered radical was formed, one hydroxide ion was formed, and the Fe^{2+} was oxidized to Fe^{3+}. In order to minimize the amount of iron required in this reaction, Fe^{3+} was reduced back to Fe^{2+} thus completing the catalytic cycle. Typical reducing agents used in this redox reaction were glucose, fructose and vitamin C.

The monosaccharide reducing sugars used in the present study were glucose, fructose, galactose and mannose. Sucrose, being a non-reducing disaccharide, was used to verify the effect of the reducing monosaccharide sugars on the polymerization process.

Evidence (including UV/VIS spectroscopy and cyclic voltammetry) in support of the reduction of Cu^{2+} to Cu^{1+} (by the monosaccharide reducing sugars) as the predominant effect responsible for the polymerization rate enhancement is also presented in this study.

1.3 Motivation

There are numerous advantages to an enhanced polymerization rate:

(a) The process could be favourable for industrial and commercial application

(b) *Economical benefits:* (1) less catalyst needed

(2) lower temperatures required

(c) *Cleaner products*

2. HISTORICAL DEVELOPMENT OF ATOM TRANSFER RADICAL POLYMERIZATION (HOMOPOLYMERIZATION)

2.1 Introduction

Matyjaszewski and Wang[4] and Sawamoto *et al.*[5] introduced the scientific community to atom transfer radical polymerization (ATRP) approximately six years ago. In 1995 Matyjaszewski and Wang showed that atom transfer radical addition (ATRA) can be successfully extended to atom transfer radical polymerization (ATRP). They used the heterogeneous initiating system 1-phenylethyl chloride/CuCl/2,2' bipyridine, in the ATRP of styrene.[4] In the same year they also reported the use of ATRP for the polymerization of methacrylates using commercially available alkyl halides combined with CuX/bipyridine (X = Cl or Br) as efficient initiating systems.[6] They furthermore successfully used the conventional radical initiator AIBN in the reverse ATRP of methyl methacrylate.[7]

In 1996 Gaynor *et al.* used ATRP for the synthesis of branched, hyperbranched and cross-linked polymers.[8, 9] In the same year the mechanistic and kinetic principles governing the ATRP system were elucidated by Paik, Matyjaszewski and Xia.[10, 11]
Since then, numerous improvements have been made to the ATRP system in terms of: the use of more effective ligands and initiators, the use of different transition metals and ways to address the issue of the associated slow polymerization rates.

Some of the advancements made in the field of ATRP are described in the following section, under (1) catalytic systems, (2) initiators, (3) reverse ATRP and (4) monomers successfully polymerized.

2.2 Recent advances in atom transfer radical polymerization

2.2.1 Catalytic systems

The efficiency of the first catalytic system reported by Sawamoto *et al* ($RuCl_2(PPh_3)_3$) was dependent on the addition of a Lewis acid ($Al(O^iPr)_3$.[5] Matyjaszewski *et al.* used the combination of Cu-salts and

bipyridine derivatives for the polymerization of styrene and methyl methacrylate, for which temperatures of 90 ^{0}C and higher were required.[4, 6, 12] The need for more efficient catalytic systems and homogeneous ATRP systems with enhanced polymerization rate (at reduced temperatures), sparked the discovery of numerous ligands capable of satisfying the aforementioned needs. A summary of these advances in the catalytic system used in ATRP is presented in Table 2.1.

Table 2.1 Summary of advances made in the catalytic systems used in ATRP

Year	Advancement	Author(s)	Ref(s)
1996	ATRP of styrene using the **Wilkinson catalyst** ($RhCl(PPh_3)_3$)	Percec *et al.*	13
1997	From heterogeneous to homogeneous catalysis using **1,10-phenantroline and its derivatives** as new copper(I) ligands	Destarac *et al.*	14
1997	ATRP of methyl methacrylate initiated by alkyl bromide and **2-pyridinecarbaldehyde imine** copper(I) complexes	Haddleton *et al.*	15
1997	(a) ATRP of styrene in the presence of **iron complexes** (b) ATRP of methyl methacrylate in the presence of **iron complexes**	Wei *et al.*	16, 17
1997	ATRP of styrene in the presence of **copper carboxylates**	Wei and Xia	18
1998	**Copper triflate** as a catalyst in ATRP of styrene and methyl acrylate	Woodworth *et al.*	19
1998	Bulk ATRP of styrene using **di-functional, tetra-functional and hexafunctional ruthenium tris(bipyridine)** reagents	Collins and Fraser	20
1998	Alternative ATRP for MMA using **$FeCl_3$** and AIBN in the presence of **triphenylphosphine**	Moineau *et al.*	21
1998	The use of **multidentate amine ligands**	Xia and Matyjaszewski	22
1998	ATRP of acrylates at ambient temperatures using **Me_6TREN** as ligand	Xia *et al.*	23
1998	ATRP of styrene using an **iron(II) complex** of a **tetradentate Schiff-base**	Wolfe and Nguyen	24
1998	Bulk ATRP of styrene using **multifunctional ruthenium(II) tris bipyridine** complexes as initiators	Collins and Fraser	25
1998	ATRP of methyl methacrylate catalyzed by **2-pyridinecarbaldehyde N-alkylimine copper (I)** complexes	Destarac *et al.*	26

1999	**4,4',4''-Tris(5-nonyl)-2,2'/6,2''-terpyridine** as ligand in ATRP	Kickelbick and Matyjaszewski	27
1999	ATRP catalyzed by copper(I) and **picolylamine** complexes	Xia and Matyjaszewski	28
1999	Copper-complexes with **quadridentate ligands** and their use as catalysts for ATRP	Ng *et al.*	29

2.2.2 Initiators

The initiators generally used in ATRP are activated alkyl halides such as ethyl 2-bromoisobutyrate, 1-phenyl ethyl bromide (or chloride), polychloroalkanes and sulfonyl chlorides.[30] These initiators often present potential drawbacks in terms of slow or multifunctional initiation, cost and toxicity.[21] Owing to the disadvantages associated with using these alkyl halide initiators, it became necessary to look at more suitable alternatives. Matyjaszewski *et al.* and also Moineau *et al.* successfully utilised the classic radical initiator AIBN in the reverse ATRP of styrene and methyl methacrylate, respectively.[7, 31, 21]

Over the last three years, various structural features of the initiators that affect the initiation efficiency have been reported. Wang *et al.* showed that ethyl 2-bromoisobutyrate is a more efficient initiator compared to its chloride counterpart due to the weaker bond strength of the C-Br bond.[32] He also reported p-toluenesulfonyl chloride to be more efficient than benzhydryl chloride (Ph_2CHCl), because p-toluenesulfonyl radicals do not terminate bimolecularly, since the formation of α, α-disulfones is relatively slow.[32, 33] Thus, they can only add to the monomer and initiate polymerization.
On the other hand, benzhydryl radicals can couple quickly to form tetraphenylethanes.

Other types of initiators that have been successfully utilised in ATRP include: allyl halide[34], functional[35] (carboxylic acid group), octafunctional[36], multifunctional star[37] and chloro-telechelic poly(ethylene oxide)S[38] initiators.

2.2.3 Reverse atom transfer radical polymerization

Wang and Matyjaszewski were amongst the first to show that the ATRP equilibrium can be approached from either side.[7] This gave rise to the so- called reverse ATRP. Reverse ATRP has the advantage that the catalyst (CuX_2) is neither air- nor moisture-sensitive as it is already in the oxidized form. It has been shown that reverse ATRP leads to the same reaction products as the classic ATRP reaction.[7, 39, 40] Wang *et al.* have shown that the classic radical initiator AIBN can be successfully used for the reverse ATRP of methyl acrylate under heterogeneous conditions.[41] Reverse ATRP has recently been extended to include the use of Fe-based catalysts.[21] Very recently (1999) Qiu et al reported the emulsion polymerization of n-butyl methacrylate by reverse ATRP.[42]

2.2.4 Monomers successfully polymerized

Most work documented on ATRP over the past six years has been on styrene, methyl methacrylate, methyl acrylate, n-butyl methacrylate and butyl acrylate. ATRP of these monomers yielded well-defined polymers with controlled molecular weights and polydispersities as low as 1.05. Qiu *et al.*[43] and Gao *et al.*[44] also reported success with substituted styrenes and 4-acetoxystyrene, respectively. Other successes include the ATRP of acrylonitrile and the following acrylates: isobornyl[45], 2-hydroxyethyl[46], glycidyl and allyl[47]. Some of the more 'exotic' monomers successfully polymerized by ATRP include 4-vinylpyridine[48], 2-(dimethylamino)ethyl methacrylate[49] and the macromonomer poly(vinyl ether)[50].

3. THEORETICAL BACKGROUND

3.1 Atom transfer radical addition

3.1.1 Mechanism of atom transfer radical addition

Atom transfer radical polymerization (ATRP) owes its existence to atom transfer radical addition (ATRA).[51] Atom transfer radical addition is a well-known method for carbon-carbon bond formation in organic synthesis. Two types of atom transfer methods have been developed. One type is called atom abstraction or homolytic substitution, in which a univalent atom, typically a halogen, is transferred from a neutral molecule to a radical species to form a new σ-bond and a new radical.[52] The other atom transfer method, which is relevant to this study, is promoted by a transition metal species.[53-58] In these reactions, the transition metal compound acts as a carrier of the halogen atom in a redox process (Scheme 3.1).[6]

Scheme 3.1 Atom Transfer Radical Addition

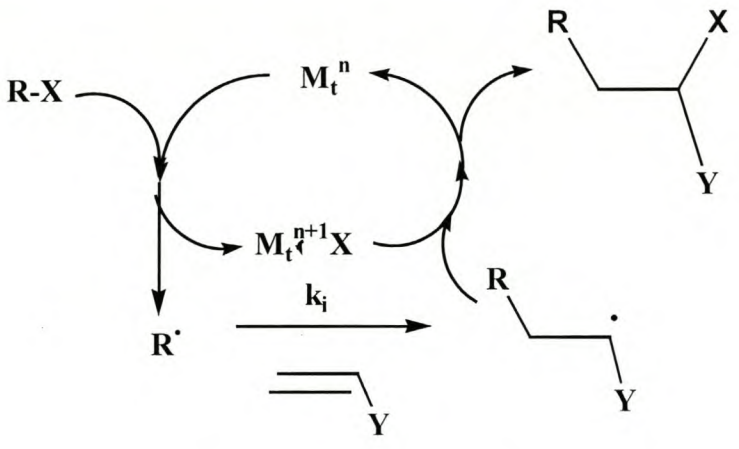

Initially, the transition metal species, M_t^n, abstracts the halogen atom X from the organic halide, R-X, to form the oxidized species, $M_t^{n+1}X$, and the carbon-centered radical R$^\bullet$. In the subsequent step, the radical, R$^\bullet$, reacts with the alkene, M, to form the intermediate radical species, R-M$^\bullet$. The reaction

between $M_t^{n+1}X$ and R-M$^{\bullet}$ results in the target product, R-M-X, and regenerates the transition metal species, M_t^n, which further reacts with R-X to start a new redox cycle.

The high efficiency of the transition metal catalyzed atom transfer reaction in producing the target product, R-M-X, suggests that the presence of such a M_t^n/M_t^{n+1} redox process can effectively induce a low concentration of free radicals, resulting in significantly reduced termination reactions between radical species.[53-58]

If polymeric halides, R-M_n-X, are reactive enough toward M_t^n and the monomer is present in excess, a number of atom transfer radical additions, i.e., a possible "living" or controlled radical polymerization, may result.[6]

3.1.2 Copper-catalyzed addition reactions and their advantages

Since 1972 several Cu^{1+}-catalyzed additions have been carried out in the industrial laboratories of Bellus *et al.*[53] The Cu^{1+}-catalyzed addition reactions include the following:

- Additions of organic polyhalides to allyl itaconates
- Additions of organic polyhalides to acrylic acid and its derivatives
- Additions of α-halosubstituted aldehydes to acrylonitrile
- Additions of derivatives of haloacetic acids to olefins
- Additions of organic polyhalides to α-methylidene carbonyl compounds

The above listed Cu^{1+}-catalyzed reactions have highlighted a number of positive aspects of these addition reactions: (a) the simplicity of the reaction system, (b) the availability of and immense variability in the reacting components, (c) the predictability of the reaction products, and (d) their high degree of latent functionality that allows considerable manipulation. All this renders the Cu^{1+}-catalyzed addition reaction an exciting and versatile synthetic tool for both laboratory and industrial scale.

3.2 Mechanistic and kinetic principles of atom transfer radical polymerization

3.2.1 Introduction

For a free radical polymerization process to qualify as a 'living' or controlled polymerization system the following practical criteria must be adhered to:

a. *The rate of polymerization ($ln\{[M]_0/[M]_t\}$) should be proportional to $t^{2/3}$.*[59] Where $[M]_0$ is the initial monomer concentration and $[M]_t$ is the residual monomer concentration at any given time during the polymerization process. In other words, the polymerization must exhibit internal first-order kinetics with respect to monomer concentration. This gives an indication that side reactions (chain termination reactions) occur to a limited extent within the system, due to the presence of a low stationary concentration of growing radicals in a fast dynamic equilibrium with the dormant species.

b. *The number average molecular weight (M_n) must increase linearly with conversion.* This means that the graph of M_n vs conversion must be linear. Thus, chain transfer reactions are negligible.

c. *Low polydispersities (much less than 1.5).* This is indicative of a narrow molecular weight distribution (controlled molecular weight) that is typical for a living system.
This ensures a controlled microstructure and hence controlled macro-properties of the resulting polymer. The necessary fast exchange between dormant (non-radical) and active (radical) species will ensure that this requirement is met. Fast initiation compared to the duration of the entire polymerization is also essential for a low polydispersity.

Atom transfer radical polymerization (ATRP) is such a controlled free radical polymerization process.

In summary, two important parameters control the livingness of ATRP: (1) the concentration of the growing radicals and (2) the exchange rate between dormant and active species. The above-mentioned parameters may in turn be affected by the nature of the transition metal, the structure and properties of the ligand and initiator, the polymerization conditions, monomer structure, etc.

3.2.2 Mechanism of atom transfer radical polymerization [4-7]

ATRP utilises a transition-metal (mainly Cu^{1+}) complex catalyst system in a dynamic equilibrium between dormant (non-radical) and active (radical) species. Scheme 3.2 gives insight into the proposed mechanism.

Scheme 3.2 Mechanism of atom transfer radical polymerization

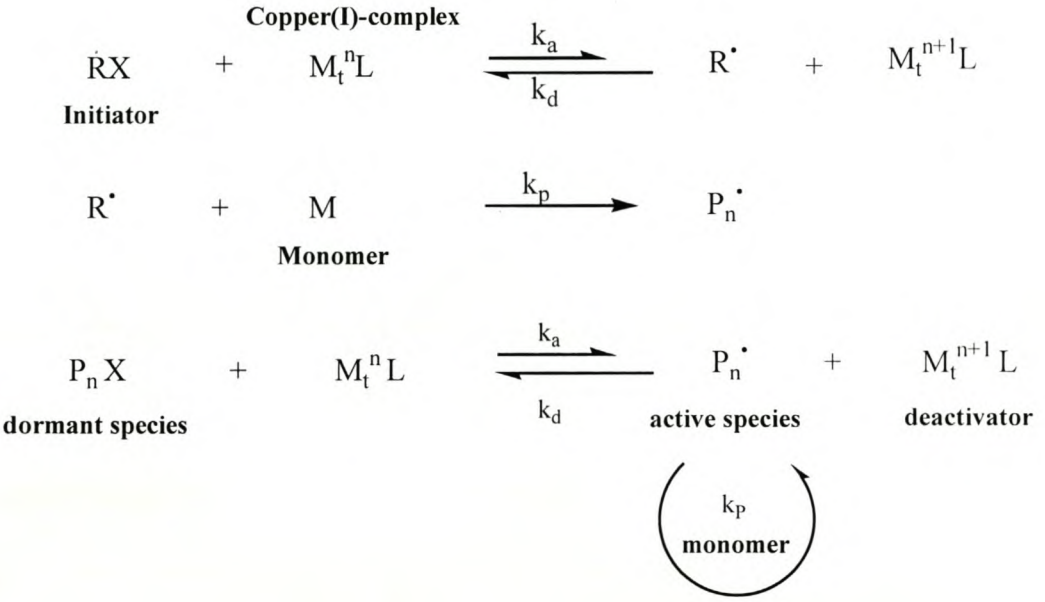

The complex, M_t^nL, acts exclusively as an atom transfer agent by abstracting the halogen atom from the inactive chain, R-X or P_nX, and forming the active radical species, $R^\bullet$ or $P_n^\bullet$. This was shown to be true by an experiment in which the complex CuBr/2dNbipy was added to free radical polymerizations of styrene (dicumyl peroxide initiator at 110 ^{0}C). Within experimental error, no effect upon the kinetics or molecular weights of the polymerization was observed. Thus, at the radical concentrations of ATRP ($\cong 10^{-7}$-10^{-8} M), the copper complex does not react with the intermediate radicals in a way that contributes to, or detracts from, the observed control of the polymerization.

3.2.3 The persistent radical effect

The following overall mechanism for the polymerization was suggested by Matyjaszewski *et al.* At the start of the polymerization the concentrations of radicals and M_t^{n+1} are zero. As the transition metal, M_t^n, reacts with the initiator, R-X, the concentration of the former two species increases. Due to the form of the equilibrium equation (Equation 3.1) and the fact that the concentrations of M_t^n and R-X are constant to within a few percent, the product of the concentrations of M_t^{n+1} and $R^\bullet$ should also be constant.

$$K_{eq} = k_a/k_d = [P^\bullet][M_t^{n+1}]/[M_t^n][R\text{-}X] \qquad (3.1)$$

where: k_a and k_d are the rate constants of activation and deactivation, respectively.

Therefore, during the initial stages of the polymerization the concentration of radicals is sufficiently large that the rate at which the radicals revert to the dormant state (rate = $k_d[M_t^{n+1}][R^\bullet]$) is much slower than the rate at which they undergo termination (rate = $k_t[R^\bullet]^2$). With each termination event, the concentration of M_t^{n+1} increases and, because the product $[M_t^{n+1}][R^\bullet]$ is constant, the concentration of radicals decreases. Therefore, the rate at which the radicals terminate decreases until a sufficient concentration of M_t^{n+1} is formed, at which point the rate of termination is slow enough for a controlled polymerization to occur. This 'self-adjustment' process during the initial stages of the polymerization is also called the 'persistent radical effect' and has been observed previously for organic radical reactions. This phenomenon also has the effect of regulating the polymerization by ensuring that the rate of radical combination and/or disproportionation is sufficiently lower than the rate of propagation.

3.2.4 Kinetics of atom transfer radical polymerization

3.2.4.1 Reaction order of each component

The kinetics of heterogeneous and homogeneous copper-catalyzed ATRP have been thoroughly investigated.[4, 31-32, 60-61, 62] Matyjaszewski *et al.* reported that the homogeneous ATRP of styrene, using 4,4'-dialkyl substituted 2,2'-bipyridines as ligands, exhibited an increase in molecular weight in direct

proportion to the ratio of the monomer consumed compared to the initial initiator concentration.[31] The above-mentioned polymerization system also exhibited internal first-order kinetics with respect to monomer, initiator and copper(I) halide concentration. However, the polymerization kinetics were not simple inverse first-order with respect to the initial copper(II) halide concentration. This was found to be due to the persistent radical effect, which resulted in an increase in the copper(II) concentration during the initial stages of the polymerization.

3.2.4.2 Factors affecting the polymerization rate

The rate of polymerization of ATRP depends upon a number of factors:

(a) *The bond strength of the C-X (X = Cl or Br) bond of the initiator.*[32]

The weaker bond correlates with a faster initiation, and hence, polymerization rate.

(b) *The different solubilities of M_t^nL and $M_t^{n+1}L$ species in various monomers and solvents.*[32]

The less $M_t^{n+1}L$ is soluble in the solvent, the faster the rate of polymerization will be (vide infra).

(c) The ligand-to-metal ratio.

It was shown by Wang *et al.* that, when using the dNbpy ligand, the polymerization rate reaches a maximum when the ligand-to-metal ratio reaches 1 for CuCl, but 2 for $CuPF_6$.[32] Matyjaszewski *et al* reported a kinetically optimum ratio of ligand-to- solubilizing 4, 4'-dialkyl substituted 2, 2' bipyridines of 2 : 1 for the homogeneous ATRP of styrene when the copper(I) halide is used.[31]

(d) *Monomer structure.*

Qiu *et al.* showed that monomers with electron-withdrawing substituents result in better polymerization control and polymerize faster than those with electron-donating substituents.[43]

3.3 Reverse atom transfer radical polymerization

3.3.1 Introduction

In a typical ATRP, the initiating system consists of an alkyl halide (R-X) and a transition metal compound in the lower oxidation state (M_t^n). The alkyl halide and M_t^n species reversibly form alkyl radicals and M_t^{n+1} species. Wang and Matyjaszewski were amongst the first to show that it is also possible to approach the same type of equilibrium starting from a conventional radical initiator, such as

AIBN, and a transition metal in its higher oxidation state (M_t^{n+1}).[7] Thus, reverse ATRP was born. It has been shown that reverse ATRP leads to the same products as the classical ATRP.[7, 39, 40] Reverse ATRP also has the added advantage that the catalyst, as it is already in the oxidized form, is neither air- nor moisture-sensitive.

3.3.2 Mechanism of reverse atom transfer radical polymerization

As mentioned in section 3.3.1, reverse ATRP employs a conventional radical initiator and a transition metal complex in its higher oxidation state. Scheme 3.3 illustrates the proposed mechanism of reverse atom transfer radical polymerization.[7]

Scheme 3.3 Mechanism of reverse atom transfer radical polymerization

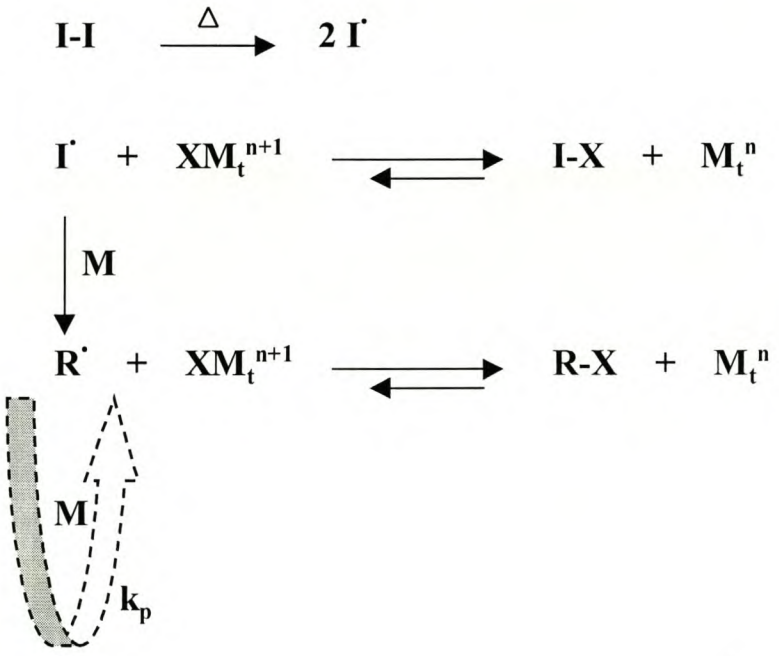

The initiation step involves the decomposition of the conventional radical initiator. The radical formed in this way can then react with the monomer to create a growing chain or react directly with the catalyst to form the reduced species M_t^n and R-X. The situation then becomes similar to the classical ATRP.

3.4 Monosaccharide reducing sugars

3.4.1 Introduction

Carbohydrates are a large family of compounds comprising the monosaccharides, oligosaccharides and polysaccharides. The monosaccharides are the simplest carbohydrates that cannot be hydrolysed further to smaller constituent units. The following section deals with the configuration of monosaccharides, their properties as it relates to certain conformational factors and their composition in solution at equilibrium.

3.4.2 Configuration of monosaccharides [63]

Monosaccharides are chiral polyhydroxy carbonyl compounds which often exist in a cyclic hemiacetal form. Monosaccharides can be divided into two main groups according to whether their acyclic form possesses an aldehyde-group (aldoses) (Figure 3.1) or keto-group (ketoses) (Figure 3.2). These, in turn, are further classified according to the number of carbon atoms (4-10) in the monomeric chain into tetroses, pentoses, hexoses, etc. and the type of functionalities (amino, sulphated, phosphorylated or deoxy saccharides) that are present.

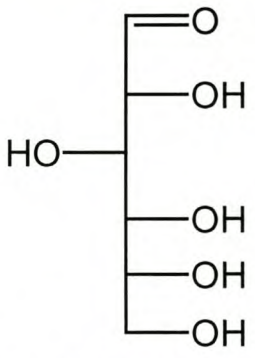

Figure 3.1 Acyclic form of D-glucose

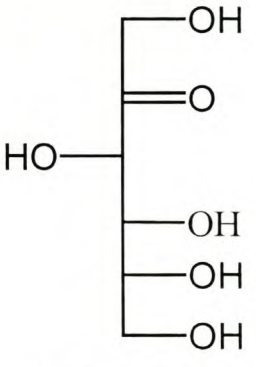

Figure 3.2 Acyclic form of D-fructose

Glucose is considered to be the parent compound of the family of monosaccharides consisting mainly of five- and six-carbon compounds. Glucose is the most abundant monosaccharide found in nature and also

the most studied one. Therefore, to get an understanding of the configuration of monosaccharides glucose is considered here as an example.

Firstly, all hexoses contain four asymmetric centres in their linear form. Therefore, $2^4 = 16$ stereoisomers exist and these can be grouped into eight pairs of enantiomers. The pairs of enantiomers are classified as D- and L-sugars. In the D-sugars, the highest numbered asymmetric hydroxyl group (C-5 in glucose) has the same configuration as the asymmetric centre in D-glyceraldehyde and, likewise, for all L-sugars the configuration is that of L-glyceraldehyde (Figure 3.3).

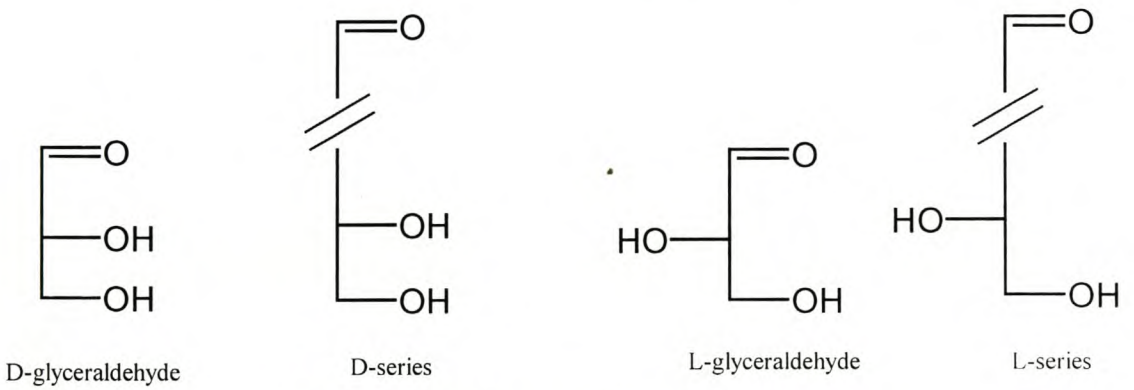

Figure 3.3 Configuration of D- and L-sugars

D-glucose exists in solution as a mixture of isomers. The linear form of glucose is energetically unfavourable relative to the cyclic hemiacetal form. The ring closure occurs by nucleophilic attack of the oxygen atom at C-5 on the carbonyl carbon atom of the acyclic species (Scheme 3.4). Hemiacetal ring formation generates a new asymmetric carbon atom at C-1, the anomeric centre, thereby giving rise to diastereoisomeric hemiacetals which are named α- and β-anomers. Cyclization involving O-4 rather than O-5 results in a five-membered ring structurally, akin to furan and is therefore designated as a furanose. Accordingly, the six-membered pyran-like monosaccharides are termed pyranoses.

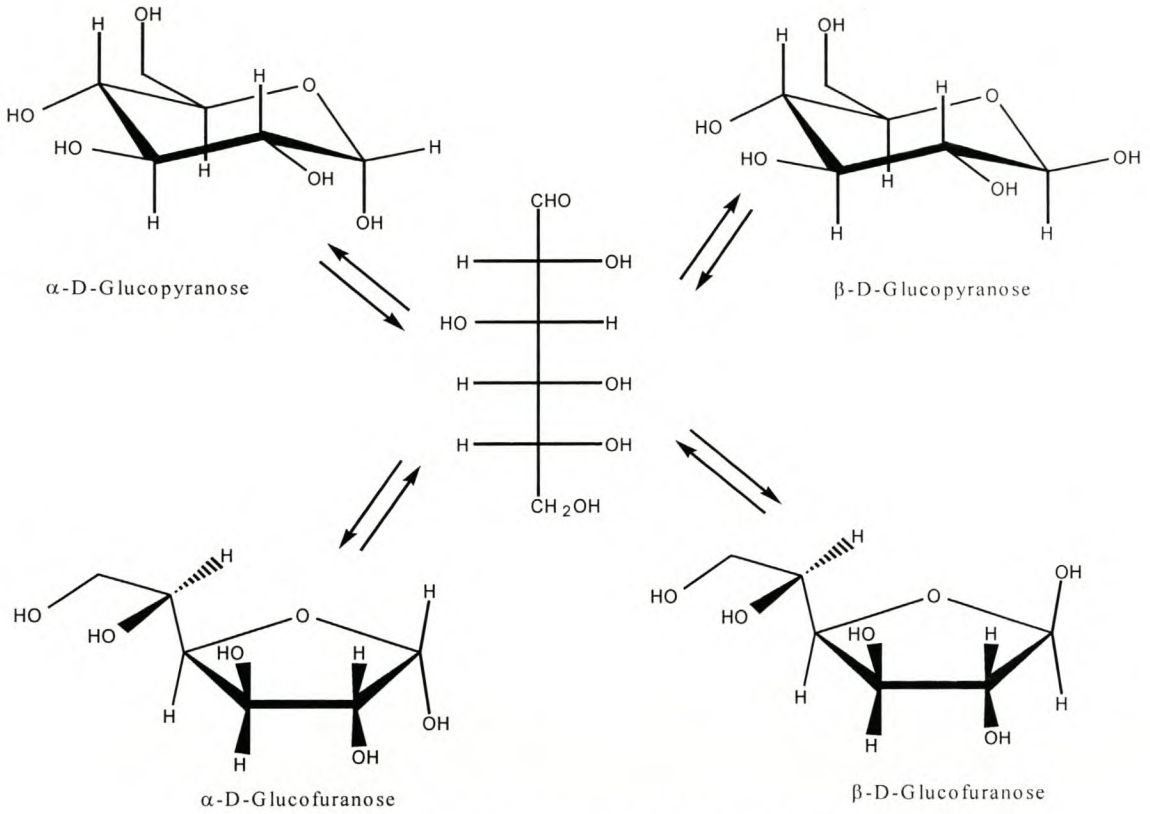

Scheme 3.4 Ring closure of acyclic glucose

3.4.3 Properties of monosaccharides in relation to conformational factors

Molecular shape seems to be the major factor on which the physical, many chemical and biochemical properties of carbohydrates depend. Equilibria involving pyranoid compounds depend largely upon the axial-equatorial relationships of substituents on the rings. Functional group reactivity also depends largely on conformation. Many reactions at the anomeric centre are dependent upon the orientation (axial or equatorial) of the group at this position. For example, equatorial anomeric hydroxyl groups of pyranoses are oxidized with aqueous bromine solution faster than when they are axial. Conversely, axial hydroxyl groups at other positions are oxidized faster with oxygen over a platinum catalyst.[64]

3.4.4 Oxidation of aldoses and ketoses [64]

Aliphatic aldehydes are readily oxidized to carboxylic acids under mild conditions, whereas ketones are more resistant. In accordance with this behaviour, aldoses are converted into aldonic acids upon

oxidation with aqueous bromine solutions over a pH range of 1 to 11. Ketoses, on the other hand, are moderately stable under the mild oxidation conditions of halogens in water. Both aldoses and ketoses yield aldonic acids when treated with Tollens reagent, which contains the complex ion $[Ag(NH_3)_2]^+$. Enediol systems derivable from α-hydroxy-ketones or –aldehydes are oxidized by Fehling's reagent, which contains blue copper(II) ions in a basic solution of sodium potassium tartrate, to give red copper (I) oxide. Due to the complexity of the oxidation, several organic products are formed in addition to aldonic acids.

3.4.5 The equilibrium composition of monosaccharides in solution [63, 64]

Both the α- and β-forms of the aldoses have a characteristic optical rotation in solution that changes with time until a constant value is reached. This change in optical rotation is called mutarotation and is indicative of molecular rearrangement occurring in solution. Aldoses and ketoses undergo rearrangements in (dilute) basic and acid solutions as a result of their hydroxycarbonyl structures. However, these sugars are significantly more stable at low pH values than in basic media.

In general, cyclic forms are heavily favoured over acyclic forms, because of the inclination of hydroxyaldehydes to cyclize. The six-membered pyranose form is preferred over the five-membered furanose form due to the relative thermodynamic stabilities of six-membered rings over five-membered analogues (Table 3.1).

Table 3.1 Composition of aldoses at equilibrium in aqueous solutions[64]

Aldose	Temperature	% Pyranose		% Furanose		Acyclic form
	(^{0} C)	α	β	α	β	(%)
Glucose	31	38	62	–	0.14	0.02
Mannose	44	64.9	34.2	0.6	0.3	0.005
Galactose	31	30	64	2.5	3.5	0.02
Fructose	31	2.5	65	6.5	25	0.8

Moreover, the equilibrium composition of monosaccharides is affected by a number of factors:

a. *Steric interactions of substituents*

The main steric interactions in a five-membered ring are between 1,2-*cis* substituents. For example, β-D-glucofuranose experiences an unfavourable interaction between the 3-hydroxyl group and the exo-cyclic side-chain (Figure 3.4). Thus, its low proportion at equilibrium (Table 3.1).

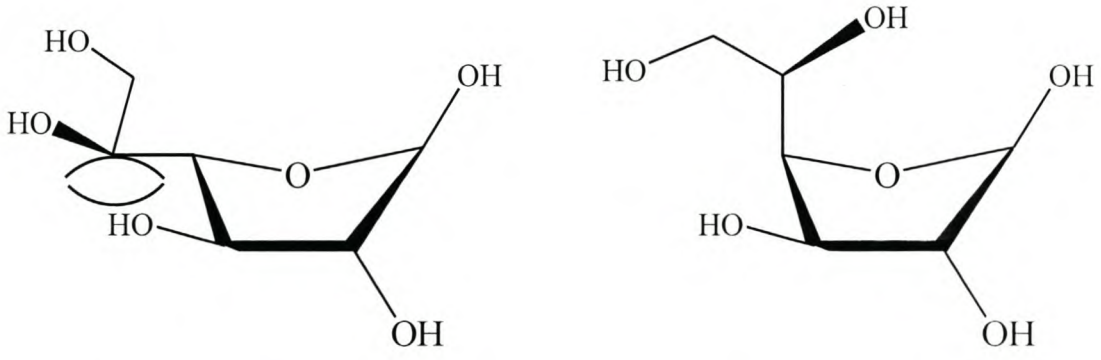

β-D-Glucofuranose β-D-Galactofuranose

Figure 3.4 Conformations of β-D-gluco- and galactofuranose

This steric interaction is absent in β-D-galactofuranose (Figure 3.4) and hence its presence, in significant quantities, at equilibrium (Table 3.1).

b. *The anomeric effect*

The anomeric effect is an orientational effect. It is the tendency of a electronegative substituent to adopt an axial orientation. Both steric factors and the anomeric effect control the α-pyranose/β-pyranose ratio. The anomeric effect is solvent dependent. It has been reported that the anomeric effect is higher in apolar solvents and hence in these apolar solvents the α-anomer is present in high proportions.

c. *The presence of particular substituents*

It has been reported that furanose proportions increase with either oxygen-substitution or removal of hydroxyl groups. Furthermore, it is known that different levels of substitution exert different degrees of α-anomerization in monosaccharides. For example, in an aqueous solution

at equilibrium, D-mannose contains 67% of the α-anomer. However, 2-O-methyl and 2,3-di-O-methyl mannose contain 75% and 86% of the α-anomer, respectively.

d. *The nature of the solvent*

The pyranose/furanose ratio also depends strongly on the nature of the solvent. It has been shown that furanose proportions increase with the addition of organic solvents. For example, in dimethyl sulphoxide (DMSO), as much as 33% arabinose exists in the furanose form, but in water this figure is merely 3%.

e. *Temperature*

An increase in temperature generally results in a decrease of the β-anomer while the proportion of α-anomer does not change and the amount of furanoses increase. For example, the furanose proportions of D-glucopyranose increase to 0.6% α and 0.7% β at 82 ^{0}C. Similarly, D-fructose comprises 10% and 32% of the α- and β-furanoses at 80 ^{0}C, respectively, and 3% of the sugar is in the form of the acyclic ketone.

3.5 Ultra violet spectroscopy

3.5.1 Introduction

As a result of energy absorption, atoms and molecules pass from a state of low energy (the ground state) to a state of higher energy (the excited state). This quantified excitation process is depicted in Figure 3.5. In the case of UV/VIS spectroscopy, the transitions that result from the absorption of electromagnetic radiation are transitions between electronic energy levels.

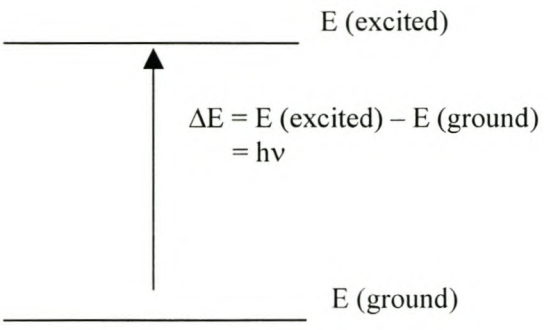

Figure 3.5 The excitation process

As a molecule absorbs energy, an electron is promoted from an occupied to an unoccupied orbital of greater potential energy. Generally, the most probable transition is from the highest occupied molecular orbital (HOMO) to the lowest unoccupied molecular orbital (LUMO).

For most molecules, the lowest-energy occupied molecular orbitals are the σ orbitals, which correspond to σ bonds. The π orbitals lie at somewhat higher energy levels. Orbitals which hold unshared electron pairs, the non-bonding (n) orbitals, lie at even higher energies. The unoccupied, or anti-bonding orbitals (π^* and σ^*), are the orbitals of highest energy. Figure 3.6 shows a typical progression of electronic energy levels and possible transitions.

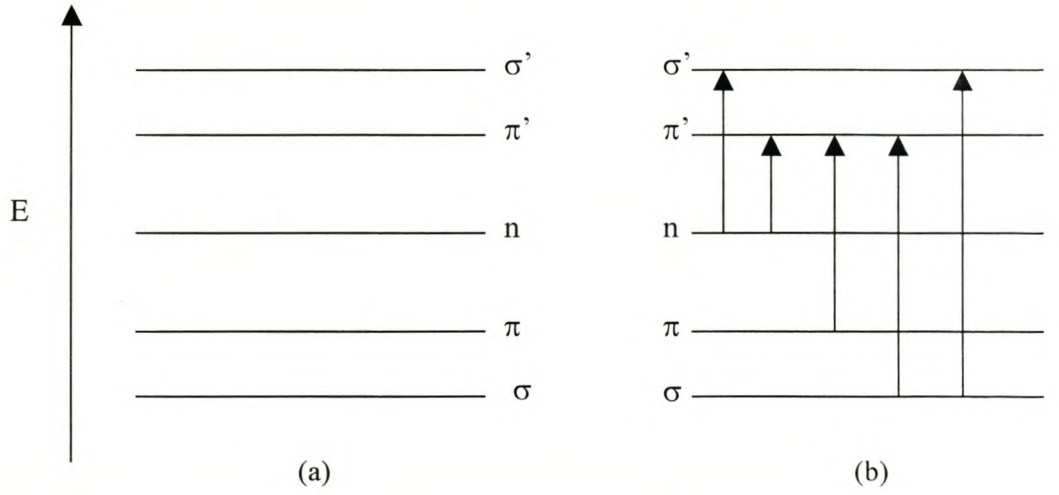

Figure 3.6 Electronic energy levels (a) and transitions (b)

The electrons may undergo several possible transitions of different energies. Some of the most important transitions are:

$\sigma \longrightarrow \sigma^*$	in alkanes
$\sigma \longrightarrow \pi^*$	in carbonyl compounds
$\pi \longrightarrow \pi^*$	in alkenes, carbonyl compounds, alkynes and azo compounds
$n \longrightarrow \sigma^*$	in oxygen, nitrogen, sulfur and halogen compounds
$n \longrightarrow \pi^*$	in carbonyl compounds

The possible transitions are governed by selection rules. For example, transitions that involve a change in the spin quantum number of an electron during the transition, are forbidden. Other selection rules deal with the number of electrons that may be excited at one time, with symmetry properties of the molecule and symmetry of the electronic states.

3.5.2 The principle of absorption spectroscopy

The principle of UV absorption is based on the Beer-Lambert Law (Equation 3.2):

$$A = \log(I_0/I) = \varepsilon c l \text{ for a given wavelength} \qquad (3.2)$$

where: A = absorbance

I_0 = intensity of light incident upon sample cell

I = intensity of light leaving sample cell

c = molar concentration of solute

l = length of sample cell (cm)

ε = molar absorptivity

The molar absorptivity is a property of the molecule undergoing an electronic transition. The size of the absorbing system and the probability that the electronic transition will take place, control the absorptivity, which ranges from 0 to 10^6. Values above 10^4 are termed high-intensity absorptions, while values below 10^3 are low-intensity absorptions. Forbidden transitions have absorptivities from 0 to 1000.

The Beer-Lambert Law is rigorously obeyed when a single species gives rise to the observed absorption. The law may not be observed under the following conditions:

- when different forms of the absorbing molecule are in equilibrium,
- when solute and solvent form complexes through some sort of association,
- when thermal equilibrium exists between the ground electronic state and a low-lying excited state, and
- when fluorescent compounds or compounds changed by irradiation are present.

3.6 Cyclic Voltammetry [65]

3.6.1 Introduction

Electrochemical techniques in which a potential (E) is imposed upon an electrochemical cell and the resulting current (i) is measured are categorized as voltammetric methods. A summary of some features of the most commonly used voltammetric methods is presented in Table 3.2. These types of voltammetry differ from one another in the type of potential waveform applied to the cell, the type of electrode used and the state of the solution in the cell (stationary or flowing). Voltammetry, in general, is very useful for analyzing dilute solutions, both qualitatively and quantitatively, of inorganic, organic and biological components, measuring thermodynamic parameters for metal-ion complexes and oxidation-reduction systems and studying the kinetics of chemical reactions.

Table 3.2 Controlled Potential Methods

Name of Techniques	Potential Excitation Signal	Mass Transfer	Measurement
Polarography (dc or normal)	Slow linear scan (or constant E)	Diffusion	i vs E
Single sweep voltammetry	Linear scan	Diffusion	i vs E
Cyclic voltammetry	***Triangular scan***	***Diffusion***	***i vs E***
Hydrodynamic voltammetry	Linear Scan	Convection or diffusion	i vs E
Stripping voltammetry	Constant E followed by linear scan	Convection or diffusion	i vs E

3.6.2 Instrumentation

The potentiostat is the main instrument used in voltammetry. The potentiostat applies a potential to the electrochemical cell between the working and reference electrodes. A current to voltage converter measures the resulting current between the working and counter electrodes. The current is typically displayed on a recorder as a function of the applied potential. Many types of voltammetry require that the potentiostat be capable of scanning from one potential to another.

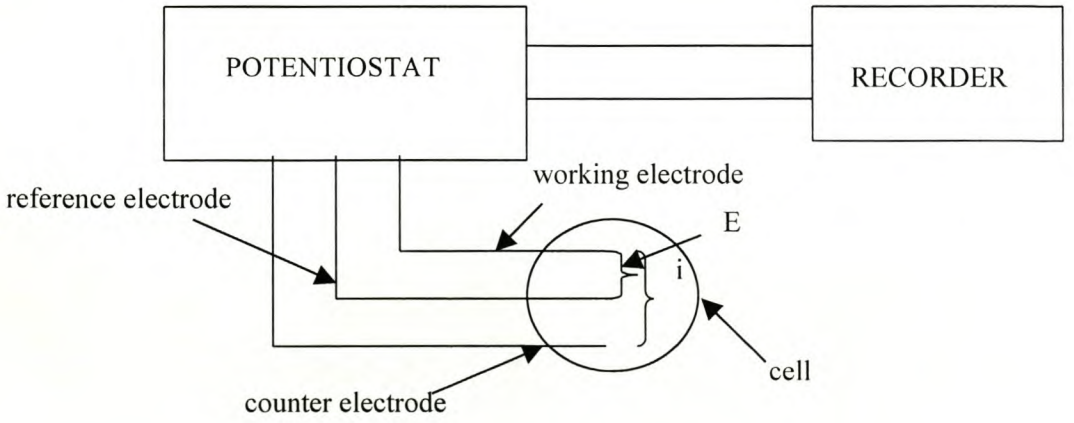

Figure 3.7 Instrumentation of voltammetry

Modern potentiostats use a three-electrode configuration, as shown in Figure 3.7. The three-electrode arrangement prevents the reference electrode from being subjected to large currents that could change its potential. Some instrumentation is based on a two-electrode system where the counter electrode is absent and the reference electrode is subjected to the entire cell current. The three-electrode system is used in this study.

The working electrode is the electrode at which the electrolysis process of interest takes place. Different types of working electrodes are utilized in voltammetry. These include the following: (a) hanging drop (usually mercury), (b) mercury film and (c) solid (platinum, gold, glassy carbon and wax-impregnated graphite) electrodes. The current required to sustain the electrolysis at the working electrode is provided by the counter electrode. The counter electrode is generally a platinum wire (coiled or uncoiled) that is often placed directly into the solution. The reference electrode is typically a saturated calomel electrode (SCE) or a Ag/AgCl electrode, which is often isolated from the solution by a tube of electrolyte called a salt bridge.

A typical electrochemical cell usually consists of a glass container with a cap having holes for introducing electrodes and nitrogen. Provision is made for oxygen removal from the solution by bubbling with nitrogen gas. The cell is then kept oxygen-free by passing nitrogen over the solution. Since the limiting (or peak) current in any type of voltammetry is temperature-dependent, the cell should be thermostated.

3.6.3 The principle of cyclic voltammetry

Cyclic voltammetry (CV) is a versatile electroanalytical technique for the study of electroactive species. The effectiveness of CV results from its capability for rapidly observing redox behaviour over a wide potential range. CV consists of cycling the potential of an electrode, which is immersed in an unstirred solution, and measuring the resulting current. The potential of this working electrode is controlled relative to a reference electrode such as a SCE or Ag/AgCl electrode. The controlling potential that is applied across these two electrodes can be considered as an excitation signal. The excitation signal for CV is a linear potential scan with a triangular waveform. The triangular potential excitation signal sweeps the potential of the electrode between two values (called the switching potentials) at a certain scan rate. Single or multiple cycles can be used. A cyclic voltammogram is obtained by measuring the current at the working electrode during the potential

scan. The current can be considered the response signal to the potential excitation signal. The voltammogram is a display of current (vertical axis) versus potential (horizontal axis).

4. EXPERIMENTAL

4.1 Atom transfer radical polymerization of n-butyl methacrylate

4.1.1 Materials

The following chemicals were used, without further purification:

- n-butyl methacrylate (n-BMA) (Aldrich), N,N,N',N",N"-pentamethyldiethylenetriamine (PMDETA) (ligand) (>99%, Aldrich),
- xylene (solvent, and internal standard for GC) (Aldrich),
- CuBr (>99%, Riedel-de Haen),
- toluene-4-sulfonyl chloride (TsCl) (initiator) (>99%, Fluka), and
- the sugars (glucose, fructose, galactose, mannose and sucrose) (Aldrich).

The molar ratios that were used were as follows:

CuBr : TsCl : PMDETA : sugar : BMA = 1 : 1 : 3 : 4 : 200.

4.1.2 Experimental procedure for the atom transfer radical polymerization of n-butyl methacrylate

Xylene, BMA, an amine ligand (PMDETA) and sugar (glucose, fructose, galactose, mannose and sucrose, respectively) were mixed together in a Schlenk-tube under an argon atmosphere. Three freeze-pump-thaw cycles were performed for oxygen removal. CuBr was added to the reaction mixture and three additional freeze-pump-thaw cycles were performed for further degassing. The reaction mixture was heated to the desired temperature (90 ^{0}C) in an oil bath before the addition of the initiator (TsCl). At
predetermined intervals (see Appendix A), samples were withdrawn from the reactor and immediately quenched by cooling in an ice-bath.

4.1.3 Characterization of poly(n-butyl methacrylate)

Monomer conversion in the above reaction was determined from the concentration of residual monomer, using xylene as internal standard. A Perkin-Elmer Autosystem XL gas chromatograph equipped with a Quadrex 15m 007 series methyl silicone column was used.

The GC conditions were as follows:

- sample volume = 0.5 μL,
- oven temperature = 80 °C,
- injector temperature = 280 °C,
- detector (FID) temperature = 300 °C
- carrier pressure = 130 kPa, and
- run time = 10 minutes.

Molecular weights and molecular weight distributions of poly(n-butyl methacrylate) were measured using a Waters SEC set up consisting of a 712 WISP autosampler; Waters 610 Fluid Unit (pump); Waters 410 Differential Refractometer (detector) and four Phenogel GPC columns (manufactured by Phenomenex) fitted in series. The pore sizes of the individual columns were 10^6, 10^5, 10^4 and 10^3 Å.

The GPC conditions were as follows:

- injection volume = 120 μL,
- solvent: THF,
- flow rate = 0.6 mL/min, and
- temperature = 30 °C.

Polystyrene standards were used to calibrate the columns. Molecular weights were recalculated to pBMA standards using the universal calibration principle and the following constants $K_{STY} = 11.4^{*}10^{-5}$ dLg^{-1}, $a_{STY} = 0.716$, $K_{BMA} = 14.8^{*}10^{-5}$ dLg^{-1}, $a_{BMA} = 0.664$.[9]

4.2 Atom transfer radical polymerization of methyl methacrylate

4.2.1 Materials

The following chemicals were used, without further purification:

- methyl methacrylate (MMA) (Aldrich), N,N,N',N",N"-pentamethyldiethylenetriamine (PMDETA) (ligand) (>99%, Aldrich),
- xylene (solvent, and internal standard for GC) (Aldrich),
- CuBr (>99%, Riedel-de Haen),
- toluene-4-sulfonyl chloride (TsCl) (initiator) (>99%, Fluka), and

- the sugars (glucose and galactose) (Aldrich).

The molar ratios that were used were as follows:

CuBr : TsCl : PMDETA : sugar : MMA = 1 : 1 : 3 : 4 : 200.

4.2.2 Experimental procedure for the atom transfer radical polymerization of methyl methacrylate

The procedure used for the synthesis of poly(methyl methacrylate) was similar to that described in section 4.1.2. Methyl methacrylate was now used rather than n-butyl methacrylate.

4.2.3 Characterization of poly(methyl methacrylate)

The characterization of poly(methyl methacrylate) was performed as described in section 4.1.3, with the exception that the calibration constants for pMMA were as follows: $K_{STY} = 11.4^{*}10^{-5}$ dLg^{-1}, $a_{STY} = 0.716$, $K_{MMA} = 12.8^{*}10^{-5}$ dLg^{-1}, $a_{MMA} = 0.697$.

4.3 Investigation of the reaction between the copper-PMDETA complex and D-glucose by ultra violet spectroscopy

4.3.1 Introduction

The aim of the ultra violet spectroscopy was to determine the type of interaction (if any) between the copper-amine complex and glucose, and thereby gain insight into the role that the monosaccharide sugars play in the observed polymerization rate enhancement.

4.3.2 Materials

The following chemicals were used, as received:

- Acetonitrile (solvent) (HPLC gradient),
- CuBr (>99%, Riedel-de Haen),
- $CuBr_2$ (>99%, Aldrich),
- N,N,N',N",N"-pentamethyldiethylenetriamine (PMDETA) (ligand) (>99%, Aldrich), and
- glucose (Aldrich).

4.3.3 Apparatus

The Perkin-Elmer Lambda 20 spectrophotometer was utilized.

4.4 Investigation of the reaction between the copper-PMDETA complex and D-glucose by cyclic voltammetry

4.4.1 Introduction

Cyclic voltammetry is very useful for the detection of species in their lower and higher oxidation states. The aim, therefore, was to investigate whether the reduction of some of the Cu(II) to Cu(I) is obtained with the addition of glucose (reducing sugar) to the Cu(II)-PMDETA complex.

4.4.2 Materials

The following chemicals were used, without further purification:

- Acetonitrile (solvent) (HPLC gradient),
- CuBr (>99%, Riedel-de Haen),
- N,N,N',N",N"-pentamethyldiethylenetriamine (PMDETA) (ligand) (>99%, Aldrich),
- glucose (Aldrich), and
- tetrabutylammoniumtetrafluoroborate ($[CH_3(CH_2)_3]_4NBF_4$) (charge carrier) (>99%, Aldrich).

4.4.3 Apparatus

The instrumentation used were the BAS CV-50W Voltammetric Analyzer, BAS Controlled Growth Mercury Electrode (CGME) and an electrochemical cell. The following electrodes were used: a mercury working electrode, a platinum counter electrode and a Ag/AgCl (saturated) reference electrode.

4.4.4 Operating conditions

Scan rate : 100 mV/s,

Sensitivity : 100 μA/V

Quiet time : 10 s.

4.4.5 Procedure

The cell was assembled and filled with 0.1 M acetonitrile so that the electrodes were immersed. The cell was deoxygenated by purging with nitrogen gas (N_2) for approximately 10 minutes. Following this, N_2 was directed over the solution to prevent oxygen from re-entering the cell during the remainder of the experiment.

5. RESULTS AND DISCUSSION

5.1 Introduction

The results obtained for the atom transfer radical polymerization of n-BMA and MMA are presented in this chapter. The results clearly show that the addition of the monosaccharide reducing sugars lead to an enhancement in the polymerization rate (sections 5.2.1 and 5.2.2). Furthermore, the investigation of the effect of the monosaccharides on the ATRP of MMA affords the opportunity to establish whether the observed phenomenon is monomer specific or not. An attempt is made to shed some light on the observed phenomenon via UV/VIS spectroscopy (section 5.3) and cyclic voltammetry (section 5.4).

5.2 The effect of various monosaccharide reducing sugars on atom transfer radical polymerization

5.2.1 Atom transfer radical polymerisation of n-butyl methacrylate

In a control experiment (no sugar added) and using PMDETA as the ligand, after 4 hours, a conversion of about 40% was observed (Figure 5.1). The addition of the reducing monosaccharides (glucose, fructose, mannose and galactose) enhanced the polymerization rate significantly. An increase in conversion of more than 100% was achieved with the addition of glucose, galactose and mannose (Figure 5.1). Sucrose, a non-reducing disaccharide, showed basically the same conversion behavior as the control reaction did (Figure 5.1). When fructose is used, extensive bimolecular termination is possible (Figure 5.2). The behavior of fructose can be ascribed to the fact that fructose is a ketose sugar (as opposed to an aldose sugar, like the other monosaccharides) (Figure 5.3).

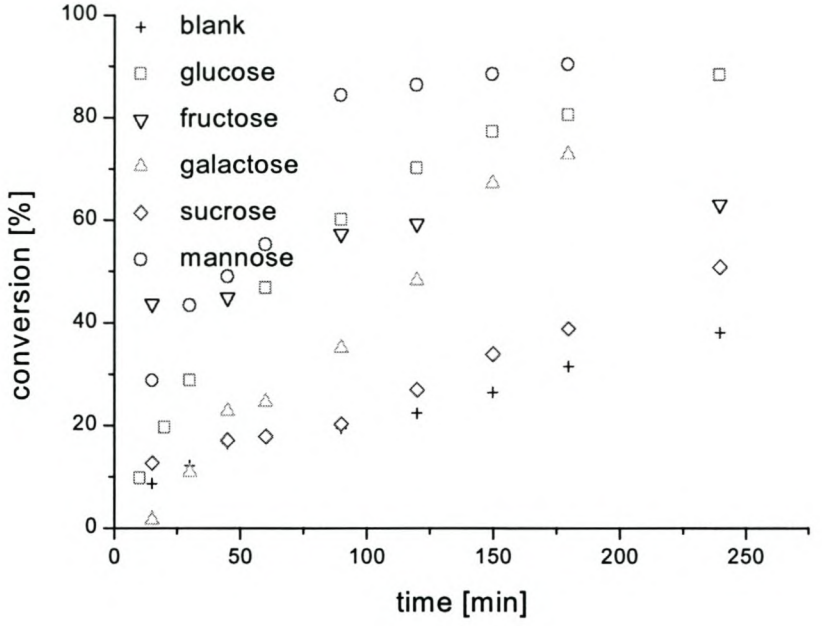

Figure 5.1 Comparison of conversion versus time for the solution (50% v/v xylene) ATRP of n-butyl methacrylate (n-BMA) using PMDETA as ligand in the presence of different sugars.
Conditions: 90 °C; Molar ratios of CuBr: TsCl: PMDETA : BMA : sugar = 1 : 1 : 3 : 200 : 4

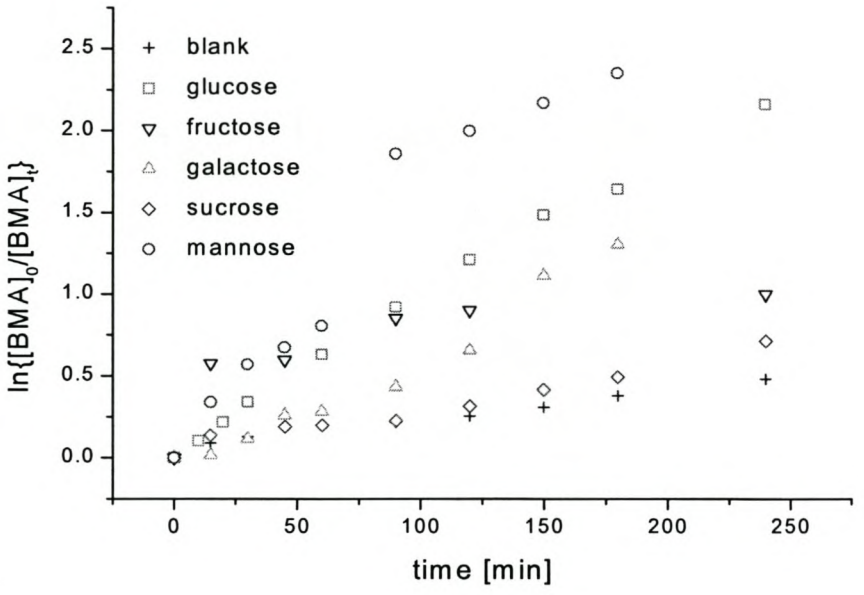

Figure 5.2 Comparison of the kinetics of the solution ATRP of n-BMA with PMDETA as ligand in the presence of different sugars.
Conditions: As for Figure 5.1.

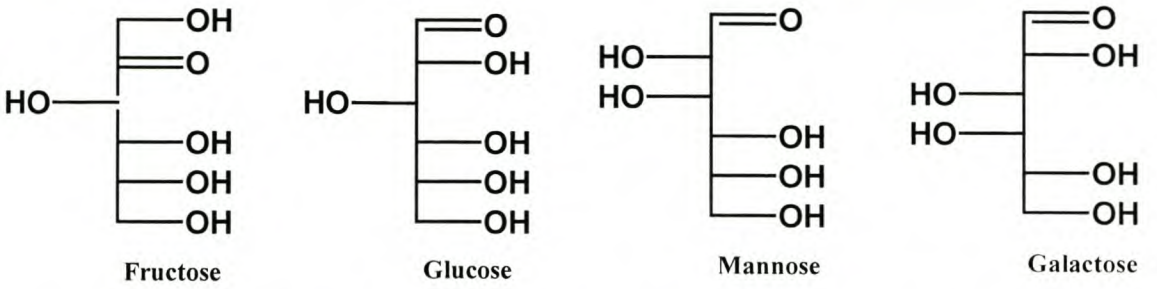

Figure 5.3 Structural formulae of the acyclic form of the monosaccharides used.

Fructose generally has a larger fraction of its acyclic form in equilibrium with its cyclic form in solution compared to the above-mentioned aldose sugars.[64] Consequently, this results in fructose being possibly more reactive (than the aldose sugars) and therefore more effective in reducing the Cu(II) species to Cu(I). It is therefore possible that this has the effect that not enough of the deactivator ($CuBr_2$) is present in the system to exercise the necessary control. A large concentration of radicals is therefore present which can lead to an increased probability of bimolecular termination. It is believed that the difference between fructose and, say, glucose is comparable to the difference between copper powder and copper turnings.[65] The too fast reduction of Cu(II) (in the cases of fructose and copper powder) leads to fast initial polymerization. This is due to the virtual absence of deactivator. This fast polymerization is uncontrolled, and in the case of fructose polymerization ceases after roughly 50% conversion due to possible (extensive) bimolecular termination. In the case of glucose and copper turnings, only the excess of Cu(II) is reduced, hence leading to an enhanced rate of polymerization but with retention of control (low polydipersities).

All measured molecular weights are greater than the theoretical values*, based upon monomer conversion and initial monomer to initiator ratio. It is expected that this deviation is due to a poor initiator efficiency. The target molecular weight for full conversion was M_n = 28,000#, which is reasonably high (low initiator concentration). Minor amounts of contamination or side reactions will cause a large deviation from the expected degree of polymerization.

---

* See Appendix B.1.2 and C.1.1
# See Appendix C.1.1

The non-linear behaviour of the molecular weights (M_n) with conversion (Figure 5.4) and the significantly higher polydispersities (M_w/M_n) (Figure 5.5) with fructose confirms the absence of control due to the high concentration of propagating radicals.

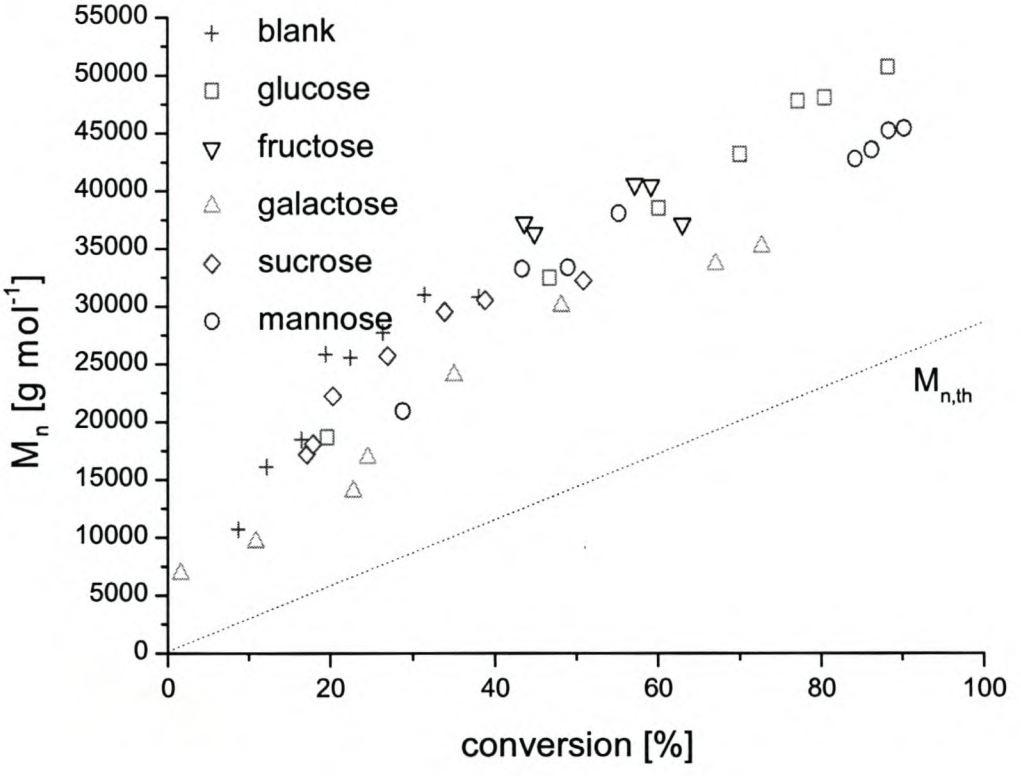

Figure 5.4 Comparison of the dependence of molecular weight (M_n) on monomer conversion for the solution ATRP of n-BMA with PMDETA as ligand in the presence of different sugars.
Conditions: As for Figure 5.1.

When glucose, galactose and sucrose are used, the M_n values increase linearly with conversion with low polydispersities (less than 1.2) throughout the polymerization (Figures 5.4 and 5.5). Some increase in polydispersity is observed at higher conversions when mannose is used. In all instances the increase in the average molecular weight with conversion remains virtually unchanged by the addition of the sugars.

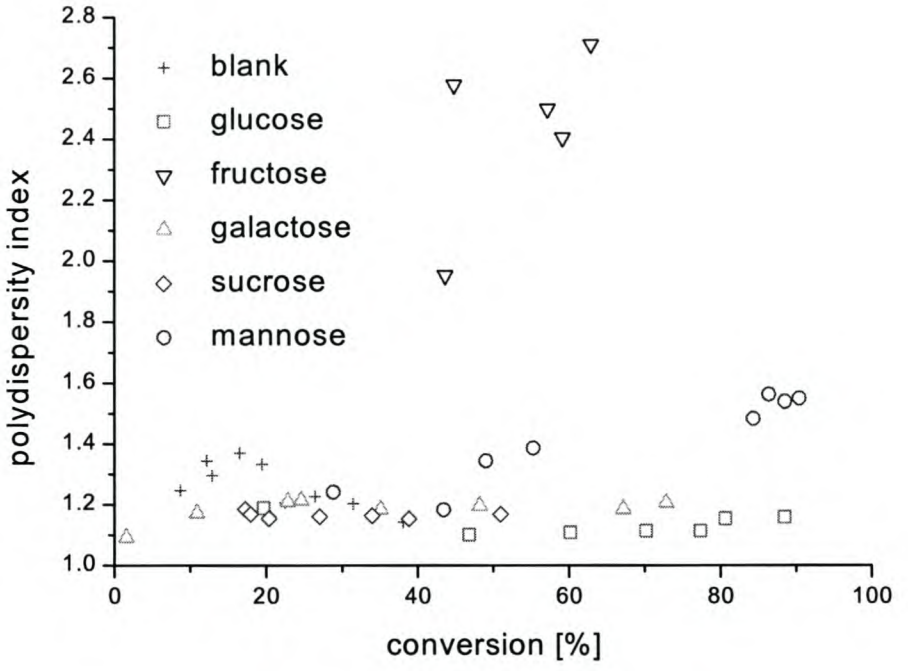

Figure 5.5 Comparison of the dependence of polydispersity (M_w/M_n) on monomer conversion for the solution ATRP of n-BMA with PMDETA as ligand in the presence of different sugars.
Conditions: As for Figure 5.1.

It is postulated, in this study, that the overall rate enhancement effect brought about by the reducing sugars is due to the reduction of Cu(II) to Cu(I) and is not an additional catalytic effect. The brownish (instead of greenish) color of the reaction mixture during polymerization, in the presence of the reducing sugars, indicates the presence of a lower [Cu(II)]. The results obtained with sucrose (non-reducing disaccharide) [Figures 5.1, 5.4 and 5.5] indicate that the reducing character of the other sugars is the key issue in their effect on the course of the polymerization.

The discussion is further supported by the fact that the Cu-PMDETA complex is very stable (stability constant, K, = 10^{12}), due to the chelate effect of the amine groups.[66] The stability of the complex is further enhanced by the positive inductive effect of the methyl groups attached to the nitrogen atoms. The possibility of ligand exchange between PMDETA and any of the sugars is therefore slight. A study of metal-carbohydrate complexes revealed that stable Cu(II) complexes cannot be expected to form with reducing sugars, which are readily oxidized by Cu(II) ions in alkaline media.[67] Moreover, Cu(II) ions are known to present a higher affinity for nitrogen than for oxygen donors, as shown by the reaction with the amino sugar taci (1, 3, 5-Triamino-1, 3, 5-

trideoxy-cis-inositol), which yields a solid compound containing $[Cu\ (taci)_2]^{2+}$ ions in which Cu(II) is bound to six nitrogen atoms.[68]

It is known that in a number of ATRP reactions hydroxyl-groups lead to an enhancement in the rate of polymerization.[69] Again, the fact that sucrose shows no effect on the rate of polymerization, and the fact that fructose shows a large increase in polymerization rate cannot be explained on the basis of the effect of the hydroxyl groups alone. Another strong indication for the postulated effect is the colour change mentioned above. Upon addition of the reducing sugars, the colour is noticeably more brownish compared to the blank experiment.

The solubility of the sugars in the organic reaction medium is low. It is not expected that solubilities of the monosaccharides in the reaction mixture will vary significantly, because of the relatively minor structural differences.

5.2.2 Atom transfer radical polymerization of methyl methacrylate

A conversion of 80 % was observed after 4 hours without any monosaccharide reducing sugar added (blank) (Figure 5.6). The same conversion was obtained with the addition of glucose and galactose after only $1^1/_2$ and 2 hours, respectively (Figure 5.6). After 4 hours the conversion reaches a maximum of approximately 93 % for glucose and 83 % for galactose.

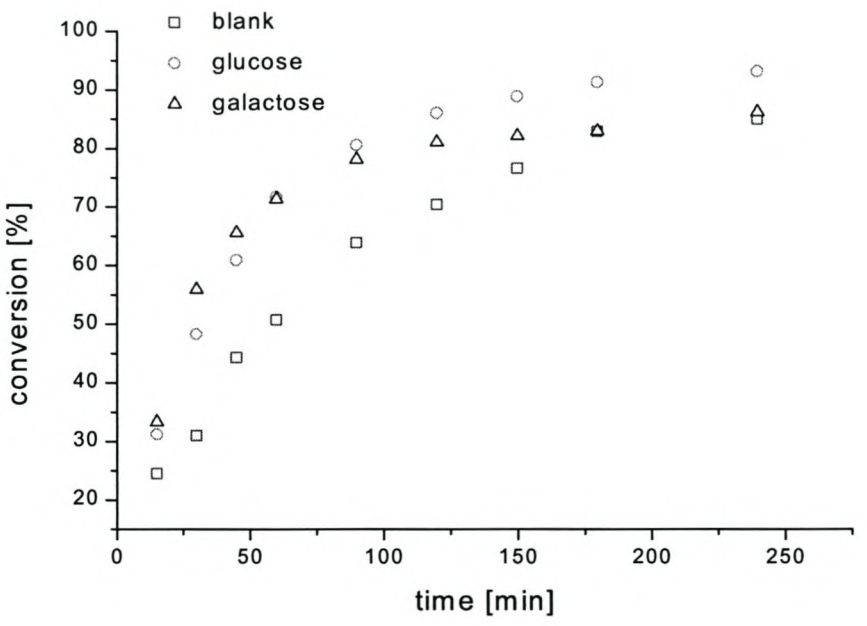

Figure 5.6 Comparison of conversion versus time for the solution (50% v/v xylene) ATRP of methyl methacrylate (MMA) using PMDETA as ligand in the presence of different sugars.
Conditions: 90 °C; Molar ratios of CuBr: TsCl: PMDETA : MMA : sugar = 1 : 1 : 3 : 200 : 4

Termination reactions seem to be more prevelant when galactose is used (Figure 5.7). This is possibly due to galactose's slightly greater ability to reduce Cu(II) to Cu(I), in the medium used, compared to glucose. This is evident in the observation of higher conversions early on in the polymerisation when galactose is used (Figure 5.6). This increased rate early on in the polymerisation with galactose, leads to the presence of greater radical concentrations and hence the increased probability of termination reactions.

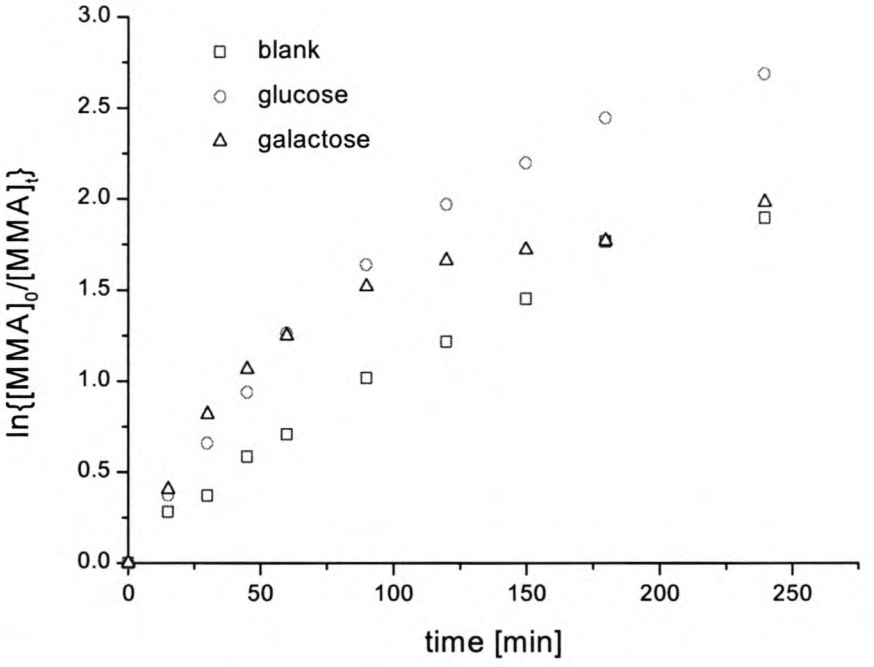

Figure 5.7 Comparison of the kinetics of the solution ATRP of MMA with PMDETA as ligand in the presence of different sugars.
Conditions: As for Figure 5.6.

The measured molecular weights increase linearly with conversion throughout the polymerisation in all cases (Figure 5.8). The M_n values for the blank reaction are lower than the expected theoretical values[♦].

Again, contamination and side reactions (in particular chain transfer reactions) can be responsible for the observed deviation from the expected degree of polymerisation. The M_n values for glucose and galactose correspond well with the theoretically expected values (Figure 5.8)[♣]. The polydispersities are below 1.1 throughout the polymerisation when no sugar is used (Figure 5.9). The addition of glucose gives polydispersities well below 1.2 up to about 75 % conversion (Figure 5.9). There is an increase in polydispersities to just above 1.2 at higher conversions. Polydispersities of about 1.2 are obtained for galactose up to approximately 65 % conversion (Figure 5.9). An increase in polydispersities to about 1.5 is observed at higher conversions for galactose. The increased

♦ See Appendix B.1.1 and C.1.2
♣ See Appendix B.1.1 and C.1.2

polydispersities at higher conversions can be ascribed to the absence of sufficient Cu(II) to exercise the necessary control over molecular weight distributions.

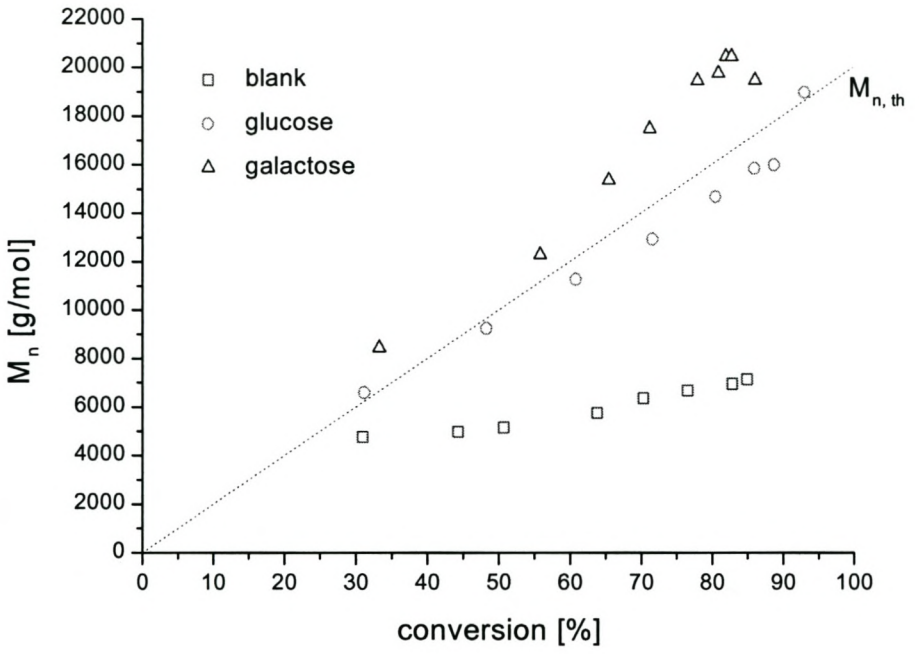

Figure 5.8 Comparison of the dependence of molecular weight (M_n) on monomer conversion for the solution ATRP of MMA with PMDETA as ligand in the presence of different sugars.
Conditions: As for Figure 5.6.

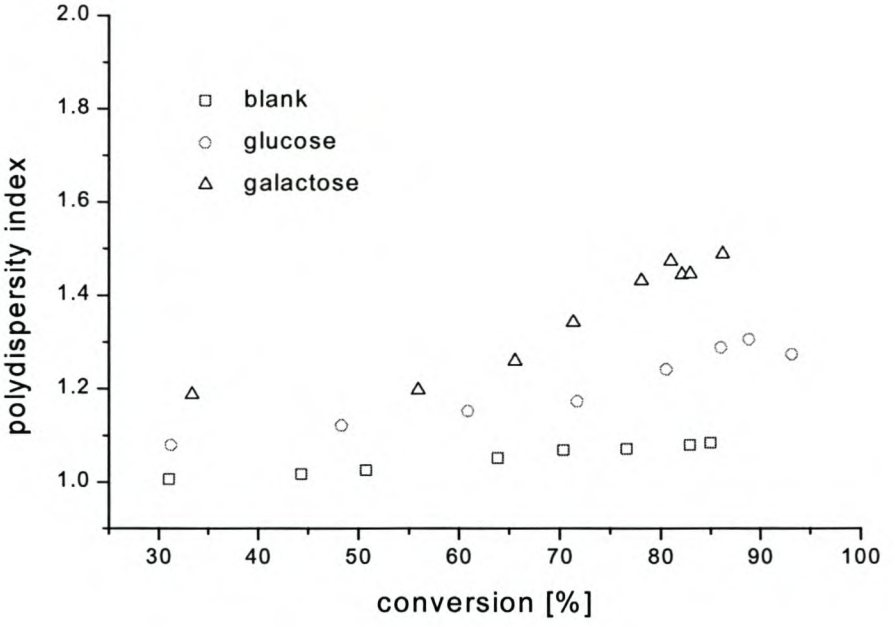

Figure 5.9 Comparison of the dependence of polydispersity (M_w/M_n) on monomer conversion for the solution ATRP of MMA with PMDETA as ligand in the presence of different sugars.
Conditions: As for Figure 5.6.

5.3 Investigation of the reaction between the copper-PMDETA complex and D-glucose by ultra violet spectroscopy

5.3.1 Objective

The aim of using ultra violet spectroscopy was to determine the type of interaction between the Cu(II)-PMDETA complex and the monosaccharide reducing sugar D-glucose. The question is: "Does the glucose form an additional inert complex with the transition metal or does it reduce some of the Cu(II) to Cu(I)?". We attempt to shed some light on this question by making use of the obtained spectrophotometric data.

5.3.2 Results and discussion

Figure 5.10 shows the individual spectra of Cu(I) and Cu(II) and the spectrum of a Cu(I)/Cu(II) reaction mixture. Figure 5.11 shows the spectrum of a reaction mixture of the Cu(I)- and Cu(II)-PMDETA complexes in the region of 220nm to 450 nm.

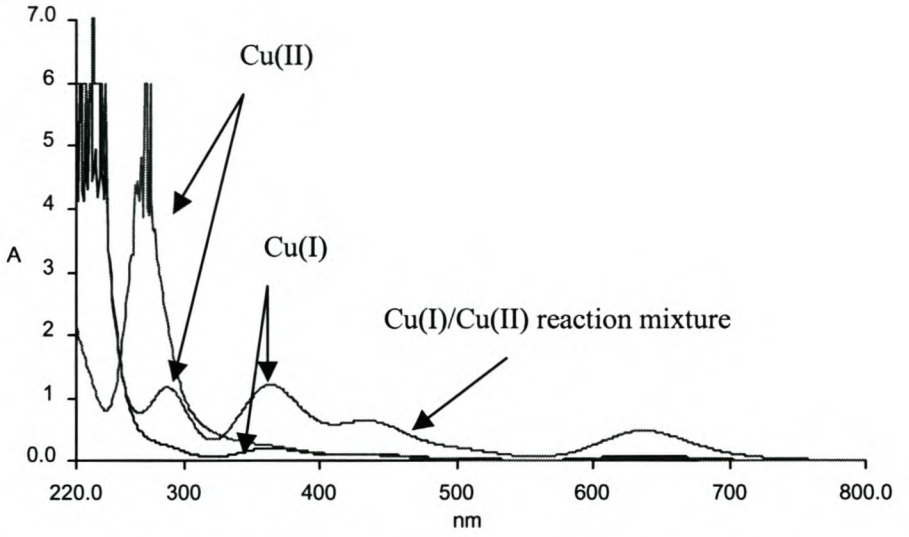

Figure 5.10 UV/VIS spectra of Cu(I), Cu(II) and a Cu(I)/Cu(II) reaction mixture.
Conditions: molar ratio of Cu(I) : Cu(II) = 1 : 1; ambient temperatures.

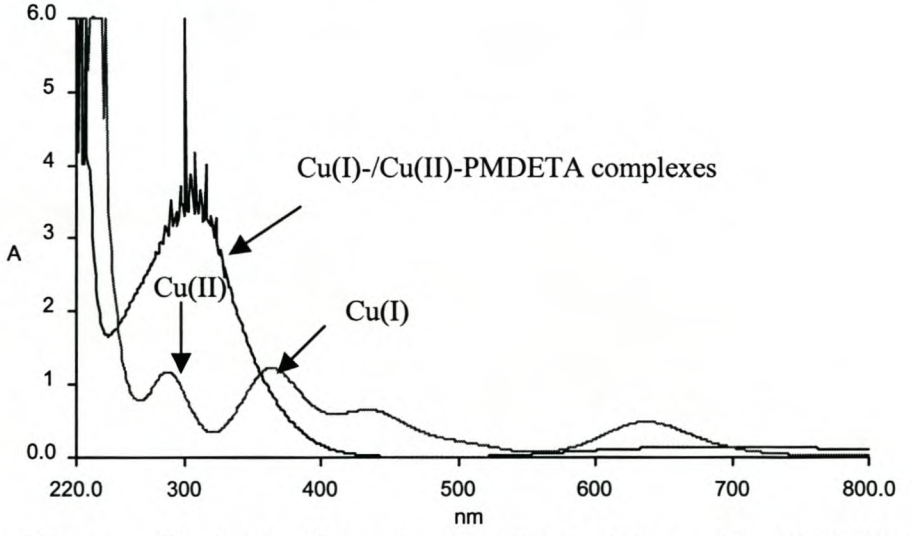

Figure 5.11 UV/VIS spectra illustrating the region in which a mixture of the Cu(I)-/Cu(II)-PMDETA complexes are observed.
Conditions: molar ratio of Cu(I) : Cu(II) : PMDETA = 1 : 1 : 2; ambient temperatures.

A definite Cu(II)-PMDETA complex is formed as indicated by an observed colour change (green to light blue) and Figure 5.12. The addition of D-glucose to the Cu(II)-PMDETA complex reaction mixture gives no additional peak, hence no inert Cu(II)-glucose complex is observed (Figure 5.13). Furthermore, a noticeable decrease in the Cu(II)-PMDETA peak height with the addition of D-glucose is observed (Figure 5.13).

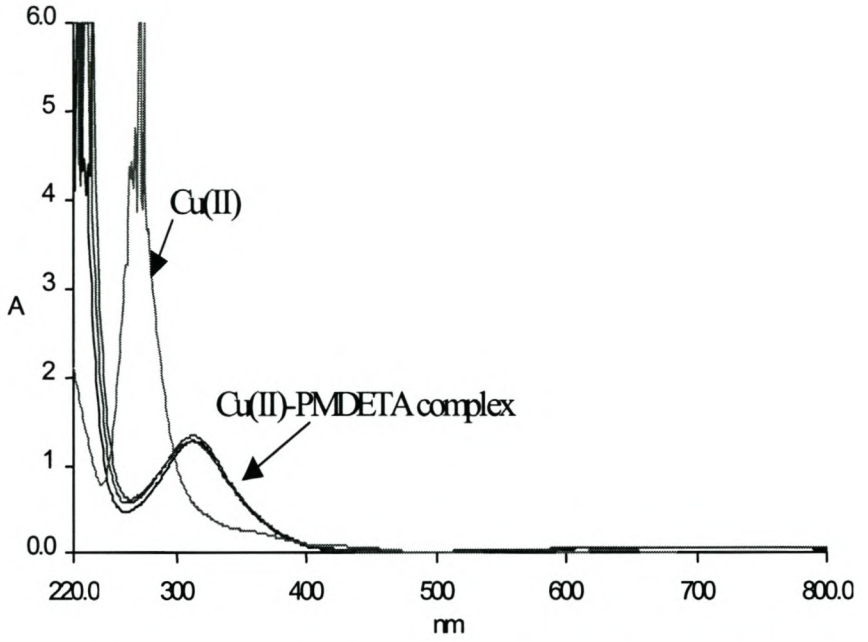

Figure 5.12 UV/VIS spectra illustrating the formation of the Cu(II)-PMDETA complex.
Conditions: molar ratios of Cu(II) : PMDETA = 1 : 1, 1 : 2 and 1 : 3; ambient temperatures.

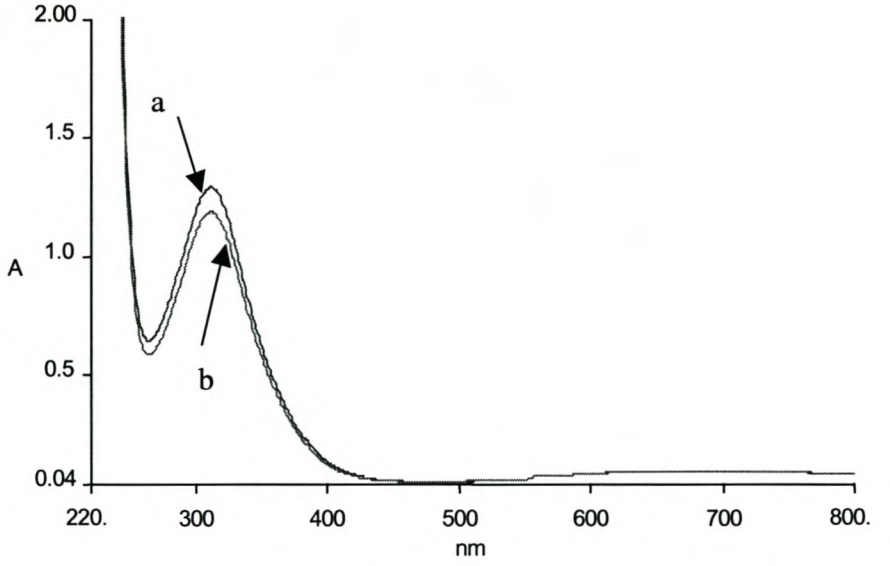

Figure 5.13 UV/VIS spectra of (a) Cu(II)-PMDETA complex and (b) Cu-PMDETA complex with D-glucose added.
Conditions: (a) molar ratio of Cu(II) : PMDETA = 1 : 3; (b) molar ratio of Cu(II) : PMDETA : D-glucose = 1 : 3 : 2♦; ambient temperatures.

♦ The solution is already saturated with D-glucose at this concentration.

The observed decrease in the Cu(II)-PMDETA peak can be due to some dissociation of the Cu(II)-PMDETA complex. The reduction of part of the Cu(II) to Cu(I) is therefore a distinct possibility. Any Cu(I) formed in this way will not be present as free metal, but in the preferred Cu(I)-PMDETA form. The possible overlapping of the Cu(I)- and Cu(II)-PMDETA complexes is observed, due to the fact that Cu(I)-PMDETA is detected in the same wavelength-range as Cu(II)-PMDETA (Figures 5.11 and 5.14).

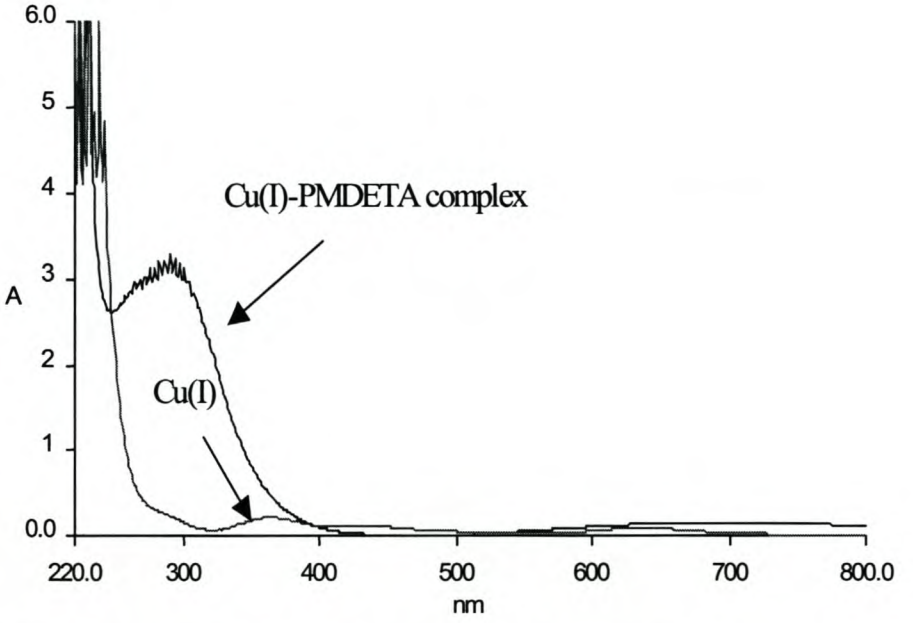

Figure 5.14 UV/VIS spectra of Cu(I) and Cu(I)-PMDETA.
Conditions: molar ratio of Cu(I) : PMDETA = 1 : 2; ambient temperatures.

5.4 Investigation of the reaction between the copper-PMDETA complex and D-glucose by cyclic voltammetry

5.4.1 Objective

The purpose of using cyclic voltammetry to investigate the reaction between the copper-PMDETA complex and D-glucose was to confirm the obtained UV spectroscopy results. If there is some dissociation of the Cu(II)-PMDETA complex taking place (as observed with the UV), then increased metal activity should be observed with the addition of D-glucose to the metal-ligand complex.

5.4.2 Results and discussion

Figure 5.15 shows the reduction-oxidation cycle of the transition metal. Strong complex formation between the copper and PMDETA is observed (Figure 5.16).

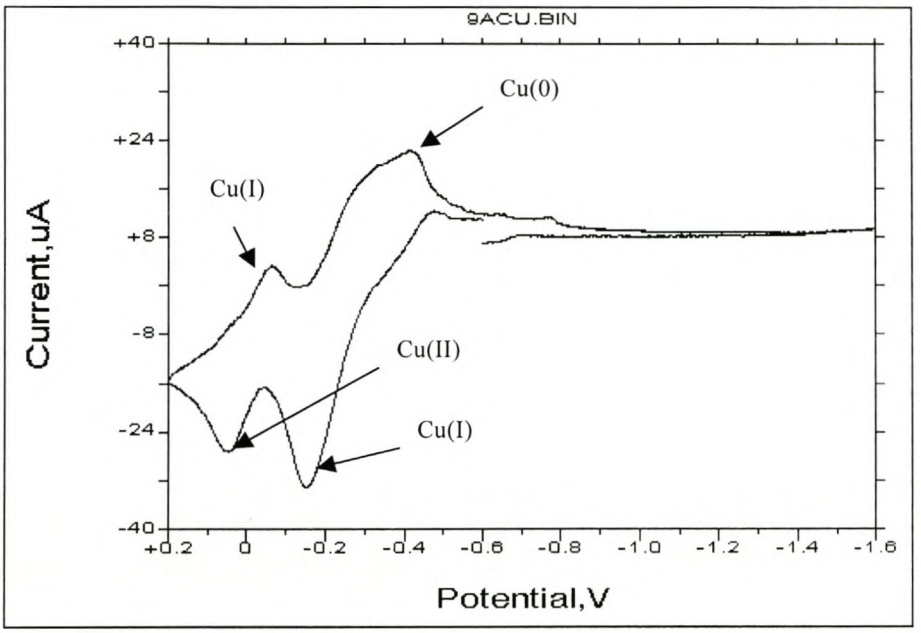

Figure 5.15 Voltammogram of the reduction-oxidation cycle of copper.

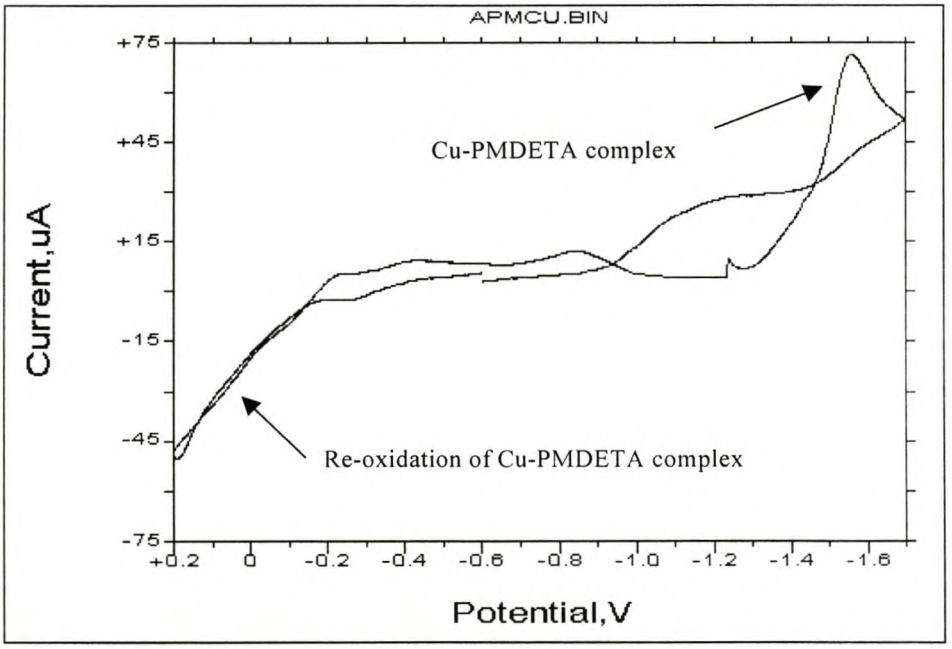

Figure 5.16 Voltammogram of the Cu-PMDETA complex. Molar ratio of Cu: PMDETA = 1 : 3.

The addition of D-glucose to the Cu-PMDETA complex results in the observation of reduction/oxidation activity in the potential region –0.1 V to -0.5 V (Figure 5.17). The activity is a clear indication that the Cu-PMDETA complex is more easily reduced and oxidized in the presence of a reducing sugar. The reduction or oxidation of the Cu-PMDETA complex is not easily observed by ultra violet spectroscopy, as the two peaks overlap (section 5.3.2)..

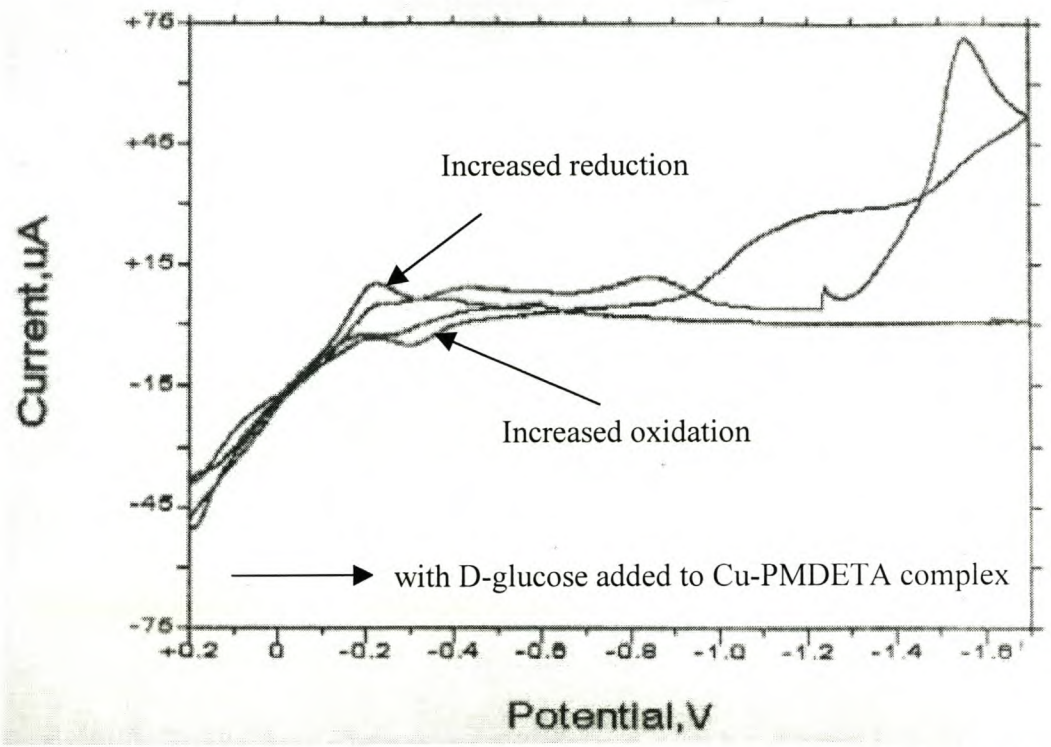

Figure 5.17 Comparison of the voltammogram of the Cu-PMDETA complex and the voltammogram of the addition of D-glucose to the Cu-PMDETA complex. Molar ratio of Cu : PMDETA : D-glucose = 1 : 3 : 2.

6. CONCLUSIONS

6.1 Conclusions

The results presented in Chapter 5 (sections 5.2.1 and 5.2.2) show that the rate of atom transfer radical polymerization of n-butyl methacrylate and methyl methacrylate can be improved by the addition of organic reducing agents such as monosaccharide reducing sugars. Furthermore, the monosaccharides are a suitable alternative for the Cu(0) that was used by Matyjaszewski *et al.*[1]

The linear increase in the molecular weight (M_n) with conversion and the low polydispersities (in most instances) throughout the polymerization indicates a controlled radical process for both n-BMA and MMA. The results obtained for the ATRP of MMA proves that the observed rate enhancement by the monosaccharide reducing sugars is not monomer specific.

The spectrophotometric (UV/VIS) (section 5.3) and cyclic voltammetry data (section 5.4) support the proposed reduction of Cu(II) to Cu(I) by the monosaccharide reducing sugars as the predominant effect responsible for the observed polymerization rate enhancement.

6.2 Recommendations

Future work should focus on the optimization of the current system in terms of the optimum copper to sugar ratio necessary for polymerization rate enhancement and adequate control over molecular weight and molecular weight distribution. Recommendations for future studies also include investigating the versatility of the observed phenomenon, the exact mechanism of the rate enhancement and the differences, in terms of solubilities, conformations and orientation of the hydroxyl groups at the anomeric position in a particular medium, among the sugars.

7. REFERENCES

1. K. Matyjaszewski, S. Coca, S.G. Gaynor, M. Wei, B.E. Woodworth, **Macromolecules**, 30, 7348 **(1997)**
2. T. Fukuda, A Goto, K. Ohno, **Macromolecular Rapid Communications**, 21, 151 **(2000)**
3. E.S. Daniels, V.L. Dimonie, M.S. El Aasser, J.W. Van der Hoff, **Journal of Polymer Science**, Polymer Chem. Ed., 41, 2463 **(1990)**
4. J.S. Wang, K. Matyjaszewski, **Journal of the American Chemical Society**, 117, 5614 **(1995)**
5. M. Kato, M. Kamigaito, M. Sawamoto, T. Higashimura, **Macromolecules**, 28, 1721 **(1995)**
6. J.S. Wang, K. Matyjaszewski, **Macromolecules**, 28, 7901 **(1995)**
7. J.S. Wang, K. Matyjaszewski, **Macromolecules**, 28, Iss. 22, 7572 **(1995)**
8. S.G. Gaynor, S.Z. Edelman, A. Kulfan, K. Matyjaszewski, **Abstracts of Papers of the American Chemical Society**, 212, Iss Aug, 149-POLY **(1996)**
9. S.G. Gaynor, S.Z. Edelman, K. Matyjaszewski, **Abstracts of Papers of the American Chemical Society**, 211, Iss Mar, 146-PMSE **(1996)**
10. H.J. Paik, K. Matyjaszewski, **Abstracts of Papers of the American Chemical Society**, 212, Iss Aug, 92-POLY **(1996)**
11. J.H. Xia, K. Matyjaszewski, **Abstracts of Papers of the American Chemical Society**, 212, Iss Aug, 164-POLY **(1996)**
12. T. Grimaud, K. Matyjaszewski, **Macromolecules**, 30, 2216 **(1997)**
13. V. Percec, B. Barboiu, A. Neumann, J.C. Ronda, M. Zhao, **Macromolecules**, 29, 3665 **(1996)**
14. M. Destarac, J..M. Bessiere, B. Boutevin, **Macromolecular Rapid Communications**, 18, Iss 11, 967 **(1997)**
15. D.M. Haddleton, C.B. Jasieczek, M.J Hannon, A.J Shooter, **Macromolecules**, 30, Iss 7, 2190 **(1997)**
16. M.L Wei, J.H. Xia, N.E. McDermott, K. Matyjaszewski, **Abstracts of Papers of the American Chemical Society**, 214, Iss Sep, 75-POLY **(1997)**
17. M.L. Wei, J.H. Xia, K. Matyjaszewski, **Abstracts of Papers of the American Chemical Society**, 214, Iss Sep, 76-POLY **(1997)**

18. M.L. Wei, J.H. Xia, **Abstracts of Papers of the American Chemical Society**, 213, Iss Apr, 319-POLY **(1997)**
19. B.E. Woodworth, Z. Metzner, K. Matyjaszewski, **Macromolecules**, 31, Iss 23, 7999 **(1998)**
20. J.E. Collins, C.L. Fraser, **Macromolecules**, 31, Iss 19, 6715 **(1998)**
21. G. Moineau, P. Dubois, R. Jerome, T. Senninger, P. Teyssie, **Macromolecules**, 31, Iss 2, 545 **(1998)**
22. J.H. Xia, K. Matyjaszewski, **Macromolecules**, 30, Iss 25, 7697 **(1998)**
23. J.H. Xia, S.G. Gaynor, K. Matyjaszewski, **Macromolecules**, 31, Iss 17, 5958 **(1998)**
24. P.S. Wolfe, S.T. Nguyen, **Abstracts of Papers of the American Chemical Society**, 216, Iss Aug, 147-POLY **(1998)**
25. J.E. Collins, C.L Fraser, **Abstracts of Papers of the American Chemical Society**, 216, Iss Aug, 157-POLY **(1998)**
26. M. Destarac, J. Alric, B. Boutevin, **Abstracts of Papers of the American Chemical Society**, 215, Iss Apr, 68-POLY **(1998)**
27. G. Kickelbick, K. Matyjaszewski, **Macromolecular Rapid Communications**, 20, Iss 6, 341 **(1999)**
28. J.H. Xia, K. Matyjaszewski, **Macromolecules**, 32, Iss 8, 2434 **(1999)**
29. C. Ng, C. Samson, C.L. Fraser, **Abstracts of Papers of the American Chemical Society**, 217, Iss Mar, 230-INOR **(1999)**
30. V. Percec, B. Barboiu, **Macromolecules**, 28, 7970 **(1995)**
31. K. Matyjaszewski, T.E. Patten, J. Xia**, Journal of the American Chemical Society**, 119, 674 **(1997)**
32. J.L. Wang., T. Grimaud, K. Matyjaszewski, **Macromolecules**, 30, 6507 **(1997)**
33. C.M.M. da Silva Correa, W.A. Waters, **Journal of the Chemical Society (C)**, 1874 **(1968)**
34. Y. Nakagawa, K. Matyjaszewski, **Polymer Journal**, 30, Iss 2, 138 **(1998)**
35. X. Zhang, J.H. Xia, S.G. Gaynor, K. Matyjaszewski, **Abstracts of Papers of the American Chemical Society**, 216, Iss Aug, 193-PMSE **(1998)**
36. S. Angot, K.S. Murthy, D. Taton, Y. Gnanou, **Macromolecules**, 31, Iss 21, 7218 **(1998)**
37. G. Kickelbick, P.J. Miller, K. Matyjaszewski, **Abstracts of Papers of the American Chemical Society**, 215, Iss Apr, 55-POLY **(1998)**
38. B. Reining, H. Keul, H. Hocker, **Polymer**, 40, Iss 12, 3555 **(1999)**
39. J.H. Xia, K. Matyjaszewski, **Macromolecules**, 30, 7692 **(1997)**
40. K. Matyjaszewski, **Macromolecules**, 31, 4710 **(1998)**

41. W.X. Wang, Z.H. Dong, P. Xia, D.Y. Yan, Q. Zhang, **Macromolecular Rapid Communications**, 19, Iss 12, 647 **(1998)**

42. J. Qiu, S.G. Gaynor, K. Matyjaszewski, **Macromolecules**, 32, Iss 9, 2872 **(1999)**

43. J. Qiu, K. Matyjaszewski, **Macromolecules**, 30, Iss 19, 5643 **(1997)**

44. B. Gao, X.Y. Chen, B. Ivan, J. Kops, W. Batsberg, **Macromolecular Rapid Communications**, 18, Iss 12, 1095 **(1998)**

45. K. Matyjaszewski, S. M. Jo, H.J. Paik, S.G. Gaynor, **Macromolecules**, 30, Iss 20, 6398 **(1997)**

46. S. Coca, K. Davis, P. Miller, K. Matyjaszewski, **Abstracts of Papers of the American Chemical Society**, 213, Iss Apr, 321-POLY **(1997)**

47. S. Coca, K. Matyjaszewski, **Abstracts of Papers of the American Chemical Society**, 213, Iss Apr, 322-POLY **(1997)**

48. J.H. Xia, X. Zhang, K. Matyjaszewski, **Abstracts of Papers of the American Chemical Society**, 216, Iss Aug, 152-POLY **(1998)**

49. X. Zhang, J.H. Xia, K. Matyjaszewski, **Abstracts of Papers of the American Chemical Society**, 216, Iss Aug, 153-POLY **(1998)**

50. K. Yamada, M. Miyazaki, K. Ohno, T. Fukuda, M. Minoda, **Macromolecules**, 32, Iss 2, 290 **(1999)**

51. (a) D.P. Curran, **Synthesis**, 489 **(1988)**
(b) D.P. Curran, **Free Radicals in Synthesis and Biology**, 37 **(1989)**
(c) D.P. Curran, **Comprehensive Organic Synthesis**, 4, 715 **(1991)**

52. (a) D.P. Curran, C.T. Chang, **Journal of Organic Chemistry**, 54, 3140 **(1989)**
(b) D.P. Curran, E. Eichenberger, M. Collis, M.G. Roepel, G. Toma, **Journal of the American Chemical Society**, 116, 4279 **(1994)**

53. D. Bellus, **Pure Applied Chemistry**, 57, 1827 **(1985)**

54. (a) H. Nagashima, **Journal of Organic Chemistry**, 58, 464 **(1993)**
(b) J.H. Udding, **Journal of Organic Chemistry**, 59, 1993 **(1994)**
(c) J. Seijas, **Tetrahedron**, 48 (9), 1637 **(1992)**

55. H. Nagashima, **Journal of Organic Chemistry**, 57, 1682 **(1992)**

56. T.K. Hayes, R. Villani, S.M. Weinreb, **Journal of the American Chemical Society**, 110, 5533 **(1988)**

57. (a) T. Hirao, **Synlett**, 217 **(1990)**
(b) T. Hirao**, Journal of Synthetic Organic Chemistry (Jpn.)**, 52 (3), 197 **(1994)**

58. J. Iqbal, B. Bhatia, N.K. Nayyar, **Chemical Reviews**, 94, 519 **(1994)**

59. H. Fischer, **Macromolecules**, 30, 5666 **(1997)**

60. A. Kajiwara, K. Matyjaszewski, M. Kamachi, **Macromolecules**, 31, Iss 17, 5695 **(1998)**

61. K. Matyjaszewski , **Macromolecules**, 31, Iss 15, 4710 **(1998)**

62. V. Percec, B. Barboiu, J.H. Kim, **Journal of the American Chemical Society**, 120, 305 **(1998)**

63. **Carbohydrate Chemistry**, Blackie Academic and Professional, an imprint of Thomson Science, First edition **(1998)**

64. P. Collins, R. Ferrier, **Monosaccharides: Their Chemistry and Their Role in Natural Products**, John Wiley and Sons Third Edition **(1998)**

65. D.T. Sawyer, W.R. Heineman, J.M. Beebe, **Chemistry Experiments for Instrumental Methods**, John Wiley and Sons **(1984)**

66. K. Matyjaszewski, J. Pyun, S.G. Gaynor, **Macromolecular Rapid Communications**, 19, 665 **(1998)**

67. Smith and Martell, **Critical Stability Constants**, Plenum (New York, N.Y.), 2, Amines, 135 **(1989)**

68. J. Verchere, S. Chapelle, S. Xiu, D.C. Crans, **Prog. Inorg. Chem.**, 47, 913 **(1998)**

69. K. Hegetschweiler, V. Gramlich, M. Ghisletta, H. Samaras, **Inorg. Chemistry**, 31, 2341 **(1992)**

70. D.M. Haddleton, A.J. Shooter, A.M. Heming, M.C. Crossman, D.J. Duncalf, S.R. Morsley, **ACS Symposium Series**, 685, 284 **(1998)**

APPENDIX A

A.1 Poly(n-butyl methacrylate)

A.1.1 Tables of conversion data

Blank

Time [minutes]	Conversion [%]
15	8.67
30	12.18
45	16.48
90	19.44
120	22.44
150	26.45
180	31.46
240	38.08

Glucose

Time [minutes]	Conversion [%]
10	9.79
20	19.64
30	28.88
60	46.80
90	60.18
120	70.18
150	77.33
180	80.61
240	88.48

Galactose

Time [minutes]	Conversion [%]
15	1.57
30	10.88
45	22.80
60	24.56
90	35.08
120	48.21
150	67.17
180	72.82

Mannose

Time [minutes]	Conversion [%]
15	28.82
30	43.42
45	49.03
60	55.32
90	84.40
120	86.45
150	88.57
180	90.47

Sucrose

Time [minutes]	Conversion [%]
15	12.69
45	17.17
60	17.90
90	20.31
120	27.00
150	33.93
180	38.85
240	50.92

Fructose

Time [minutes]	Conversion [%]
15	43.69
45	44.92
90	57.29
120	59.31
240	63.10

A.1.2 Tables of kinetic data

Blank

Time [minutes]	$Ln\{[BMA]_0/[BMA]_t\}$
15	0.090729436
30	0.129827066
45	0.180032256
90	0.216189676
120	0.254084129
150	0.307224911
180	0.377715733
240	0.479299845

Glucose

Time [minutes]	$Ln\{[BMA]_0/[BMA]_t\}$
10	0.103033993
20	0.218714125
30	0.340737871
60	0.631110765
90	0.920694729
120	1.210038530
150	1.483999418
180	1.640564573
240	2.160763139

Galactose

Time [minutes]	$Ln\{[BMA]_0/[BMA]_t\}$
15	0.015854096
30	0.115229554
45	0.258800086
60	0.281849065
90	0.431989026
120	0.658020125
150	1.113799966
180	1.302700872

Mannose

Time [minutes]	$Ln\{[BMA]_0/[BMA]_t\}$
15	0.339951543
30	0.569511851
45	0.673843677
60	0.805613061
90	1.857613412
120	1.998619589
150	2.168954875
180	2.350998452

Sucrose

Time [minutes]	Ln{[BMA]$_0$/[BMA]$_t$}
15	0.135740742
45	0.188430680
60	0.197224742
90	0.226971042
120	0.314642496
150	0.414431271
180	0.491823889
240	0.711740369

Fructose

Time [minutes]	Ln{[BMA]$_0$/[BMA]$_t$}
15	0.574215134
45	0.596295129
90	0.850685008
120	0.899157878
240	0.996879198

A.2 Poly(methyl methacrylate)

A.2.1 Tables of conversion data

Blank

Time [minutes]	Conversion [%]
15	24.52
30	31.01
45	44.34
60	50.76
90	63.89
120	70.39
150	76.63
180	82.93
240	85.00

Glucose

Time [minutes]	Conversion [%]
15	31.23
30	48.33
45	60.90
60	71.74
90	80.60
120	86.07
150	88.90
180	91.35
240	93.21

Galactose

Time [minutes]	Conversion [%]
15	33.33
30	55.93
45	65.59
60	71.38
90	78.14
120	81.06
150	82.15
180	82.98
240	86.24

A.2.2 Tables of kinetic data

Blank

Time [minutes]	$Ln\{[MMA]_0/[MMA]_t\}$
15	0.281259209
30	0.371257489
45	0.585919735
60	0.708481690
90	1.018517200
120	1.217219720
150	1.453701163
180	1.767851611
240	1.897222785

Glucose

Time [minutes]	$Ln\{[MMA]_0/[MMA]_t\}$
15	0.374402583
30	0.660292844
45	0.939047719
60	1.263722809
90	1.639897120
120	1.971125398
150	2.198225078
180	2.447610865
240	2.689719244

Galactose

Time [minutes]	$Ln\{[MMA]_0/[MMA]_t\}$
15	0.405415109
30	0.819390907
45	1.066822966
60	1.251064412
90	1.520511703
120	1.663894098
150	1.723166678
180	1.770781063
240	1.983404353

APPENDIX B

B.1 Recalculation of Molecular Weights

Having used poly(styrene) (pSty) standards for the calculation of the molecular weights of poly(n-butyl methacrylate) (pBMA) and poly(methyl methacrylate) (pMMA) via GPC, the molecular weights were recalculated here to pBMA and PMMA standards, using the universal calibration principle.[9]

Raw calculation:

1: pSty

2: pMMA

Equation: $[\eta] = KM^a$

$[\eta]_1 M_1 = [\eta]_2 M_2$

$K_1 M_1^{\alpha} M_1 = K_2 M_2^{\beta} M_2$

$K_1 M_1^{\alpha+1} = K_2 M_2^{\beta+1}$

Thus,

$M_2 = \{[K_1 M_1^{\alpha+1}]^{(1/(\beta+1))}\}/K_2$

$= \{[(11.4\text{x}10^{-5})(4566)^{0.716+1}]/12.8\text{x}10^{-5}\}^{1/(0.697+1)}$

$= 4686.68 \cong 4687$ #

B.1.1 Poly(methyl methacrylate) standards

Blank

Conversion [%]	M_n(pSty) [g/mol]	M_n(pMMA) [g/mol]
31.01	4566	4687 #
44.34	4972	5108
50.76	5150	5293
63.89	5746	5913
70.39	6367	6560
76.63	6699	6906
82.93	6987	7206
85.00	7134	7359

Glucose

Conversion [%]	M_n(pSty) [g/mol]	M_n(pMMA) [g/mol]
31.23	6598	6800
48.33	9195	9512
60.90	11290	11706
71.74	12969	13468
80.60	14616	15199
86.07	15838	16485
88.90	15889	16538
93.21	17967	18727

Galactose

Conversion [%]	M_n(pSty) [g/mol]	M_n(pMMA) [g/mol]
33.33	8443	8726
55.93	12283	12748
65.59	15310	15929
71.38	17348	18075
78.14	19232	20061
81.06	19545	20391
82.15	19994	20865
82.98	20100	20976
86.24	19458	20299

B.1.2 Poly(n-butyl methacrylate) standards

Blank

Conversion [%]	M_n(pSty) [g/mol]	M_n(pBMA) [g/mol]
8.67	9405	10700
12.18	13987	16112
16.48	15953	18453
19.44	22105	25830
22.44	21879	25558
26.45	23669	27717
31.46	26371	30986
38.08	26224	30808

Glucose

Conversion [%]	M_n(pSty) [g/mol]	M_n(pBMA) [g/mol]
19.64	16128	18661
46.80	27586	32459
60.18	32550	38499
70.18	36375	43172
77.33	40121	47764
80.61	40350	48046
88.48	42505	50694

Mannose

Conversion [%]	M_n(pSty) [g/mol]	M_n(pBMA) [g/mol]
28.82	18005	20905
43.42	28230	33241
49.03	28327	33359
55.32	32184	38052
84.40	36034	42755
86.45	36678	43543
88.57	38024	45192
90.47	38186	45391

Galactose

Conversion [%]	M_n(pSty) [g/mol]	M_n(pBMA) [g/mol]
1.57	6136	6889
10.88	8488	9626
22.8	12191	13983
24.56	14646	16896
35.08	20601	24020
48.21	25591	30041
67.17	28557	33638
72.82	29797	35145

Sucrose

Conversion [%]	M_n(pSty) [g/mol]	M_n(pBMA) [g/mol]
17.17	14886	17181
17.90	15637	18076
20.31	19098	22215
27.00	21985	25686
33.93	25157	29516
38.85	25983	30516
50.92	27405	32240

Fructose

Conversion [%]	M_n(pSty) [g/mol]	M_n(pBMA) [g/mol]
43.69	31498	37216
44.92	30757	36314
57.29	34238	40559
59.31	34130	40427
63.10	31426	37128

APPENDIX C

C.1 Expected theoretical values of the number-average molecular weights (M_n) for poly(n-butyl methacrylate) and poly(methyl methacrylate)

C.1.1 Poly(n-butyl methacrylate)

Raw calculation:

M_n (theoretical) = ($\Delta[M]/[I]_0$) x M_r x conversion

Where [M] is the monomer concentration, $[I]_0$ is the initial initiator concentration and M_r is the monomer molecular weight.

Example:

M_n = (200/1) x 142 x 0.5

= 14200 g/mol #

Conversion [%]	Theoretical M_n [g/mol]
10	2840
25	7100
50	14200#
75	21300
100	28400

C.1.2 Poly(methyl methacrylate)

Conversion [%]	Theoretical M_n [g/mol]
10	2000
25	5000
50	10000
75	15000
100	20000

APPENDIX D

D.1 Graphs of the comparison of different ratios of copper(I)bromide to sugar in the atom transfer radical polymerization of n-butyl methacrylate

D.1.1 Graph of the percentage conversion versus time

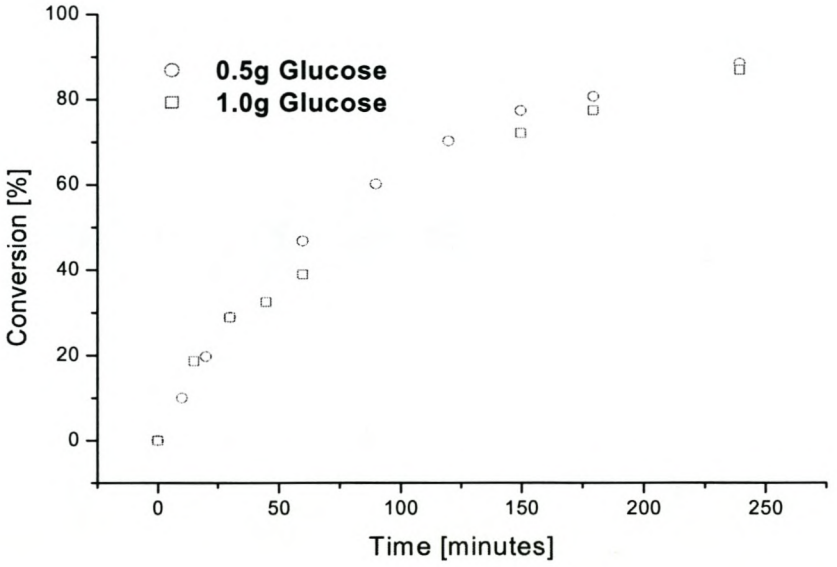

Figure 5.1 Comparison of conversion versus time for the solution (50% v/v xylene) ATRP of n-butyl methacrylate (n-BMA) using PMDETA as ligand in the presence of different ratios of glucose. Conditions: 90 °C; Molar ratios of CuBr: TsCl: PMDETA : BMA : sugar = 1 : 1 : 3 : 200 : 4 or 8

D.1.2 Graph of $ln\{[BMA]_0/[BMA]_t$ versus time

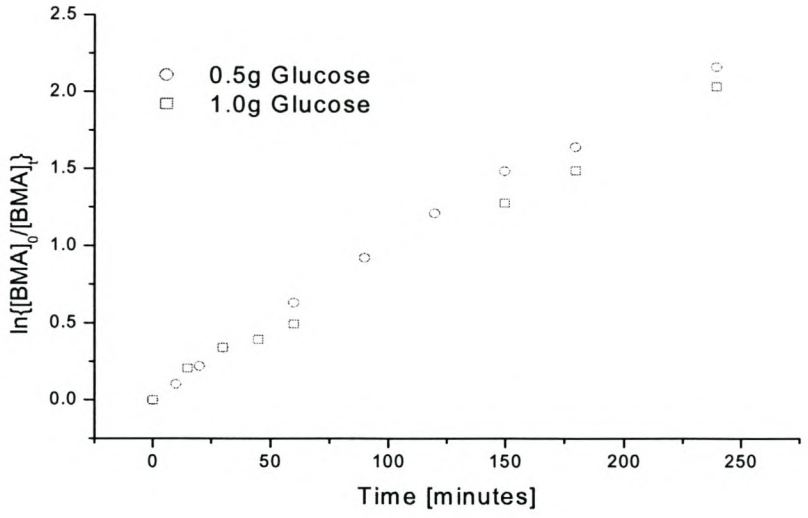

Comparison of the kinetics of the solution ATRP of n-BMA with PMDETA as ligand in the presence of different sugars. Conditions: As above.

D.1.3 Graph of the number average molecular weight versus percentage conversion

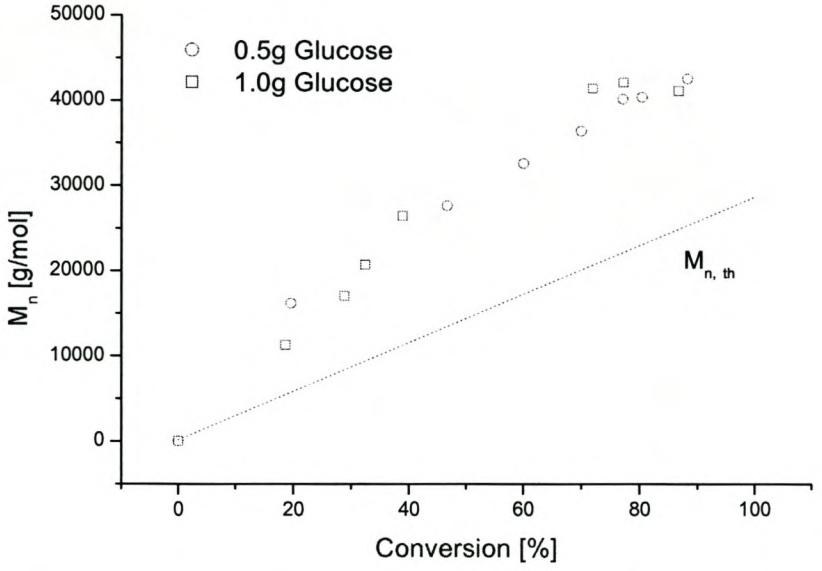

Comparison of the dependence of molecular weight (M_n) on monomer conversion for the solution ATRP of n-BMA with PMDETA as ligand in the presence of different ratios of glucose.
Conditions: As above.

APPENDIX E

E.1 Nuclear magnetic resonance (NMR) spectra of poly(n-butyl methacrylate) (The Cu-PMDETA complex was used as catalyst in the polymerization)

E.1.1 Proton NMR of poly(n-butyl methacrylate)

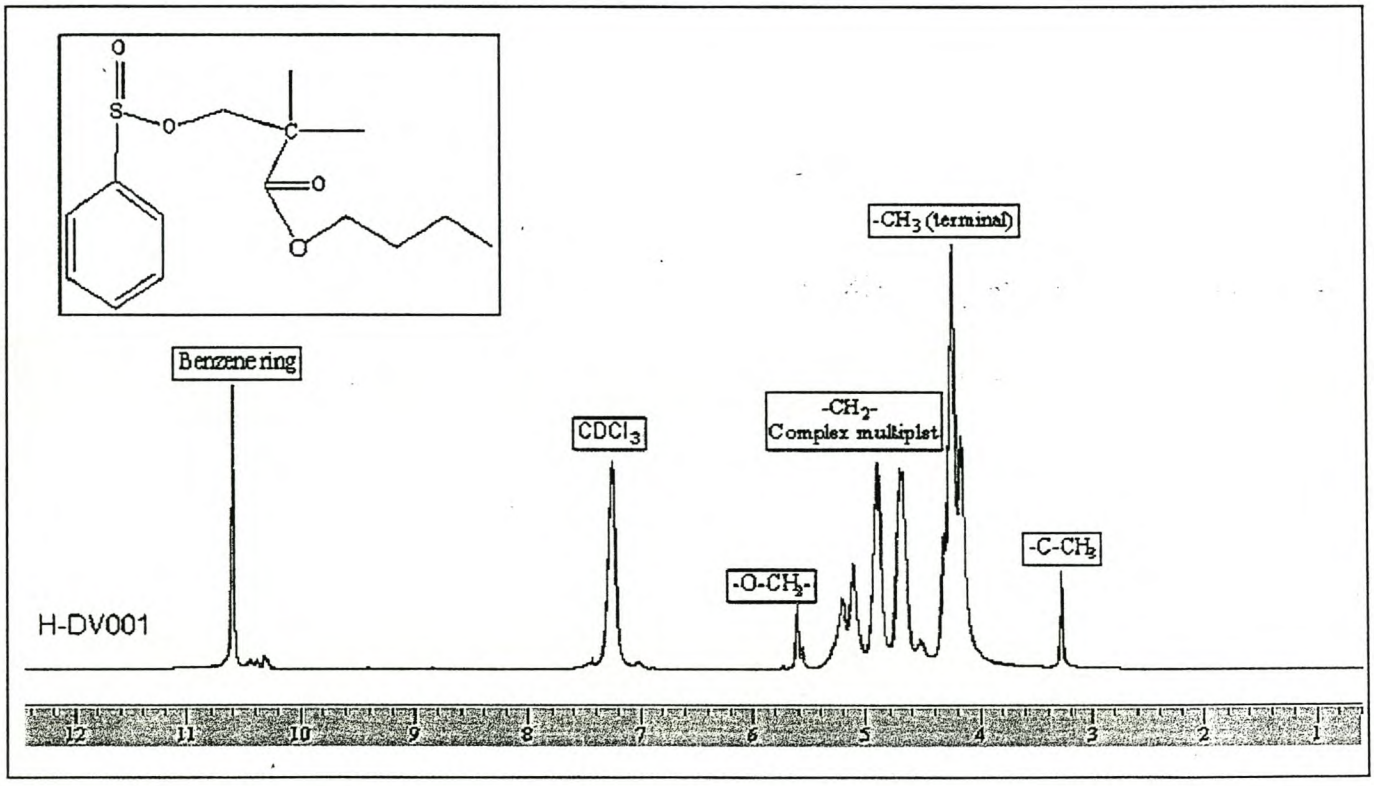

Node	Chemical shift [ppm]
Benzene ring	10.60
$CDCl_3$	7.27
-O-CH_2-	5.61
-CH_2-	4.90
-CH_3	4.25
-C-CH_3	3.30

E.1.2 Carbon-13 NMR of poly(n-butyl methacrylate)

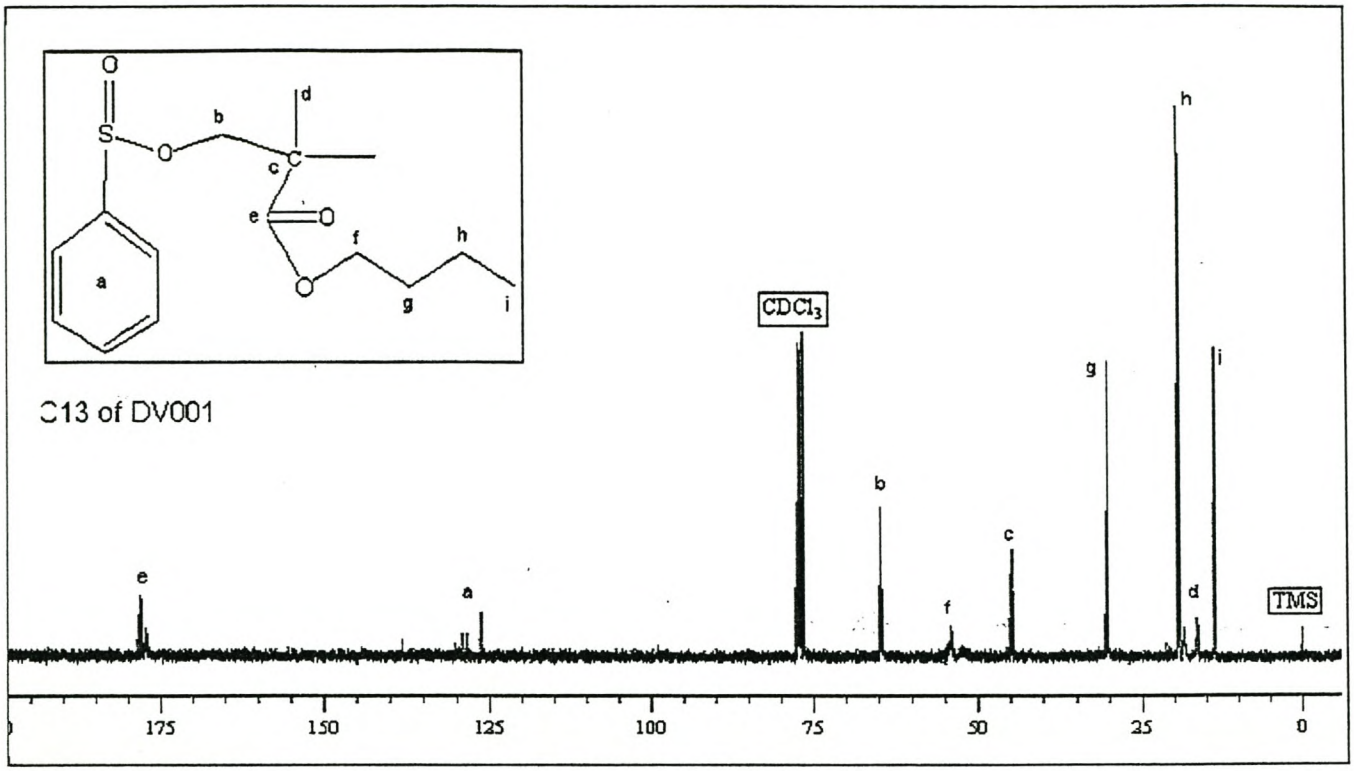

Node	Chemical shift [ppm]
a	128.25
b	64.70
c	44.99
d	17.40
e	177.72
f	53.93
g	30.01
h	19.24
i	13.46
$CDCl_3$	76.99

E.1.3 Attached proton test (APT) of poly(n-butyl methacrylate)

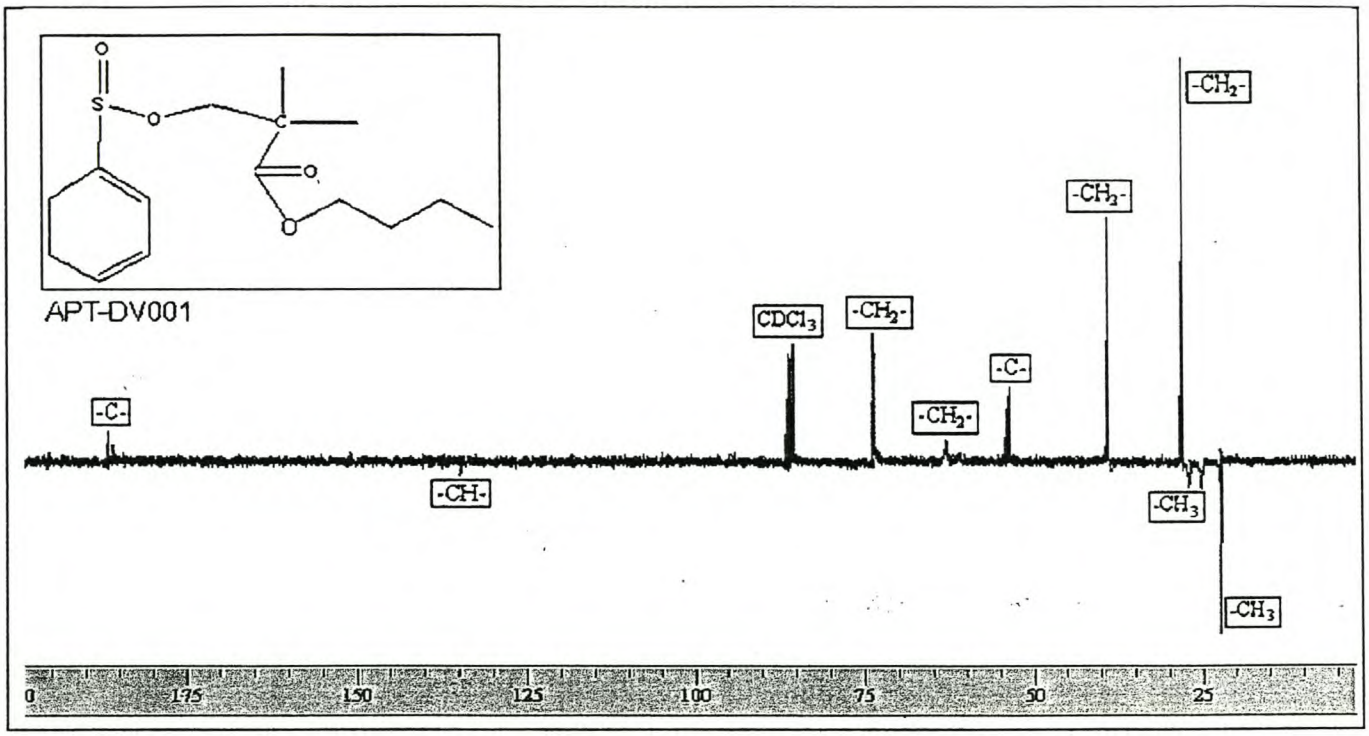

E.2 Nuclear magnetic resonance (NMR) spectra of poly(n-butyl methacrylate) (The Cu-TMEDA complex was used as catalyst in the polymerization)

E.2.1 Proton NMR of poly(n-butyl methacrylate)

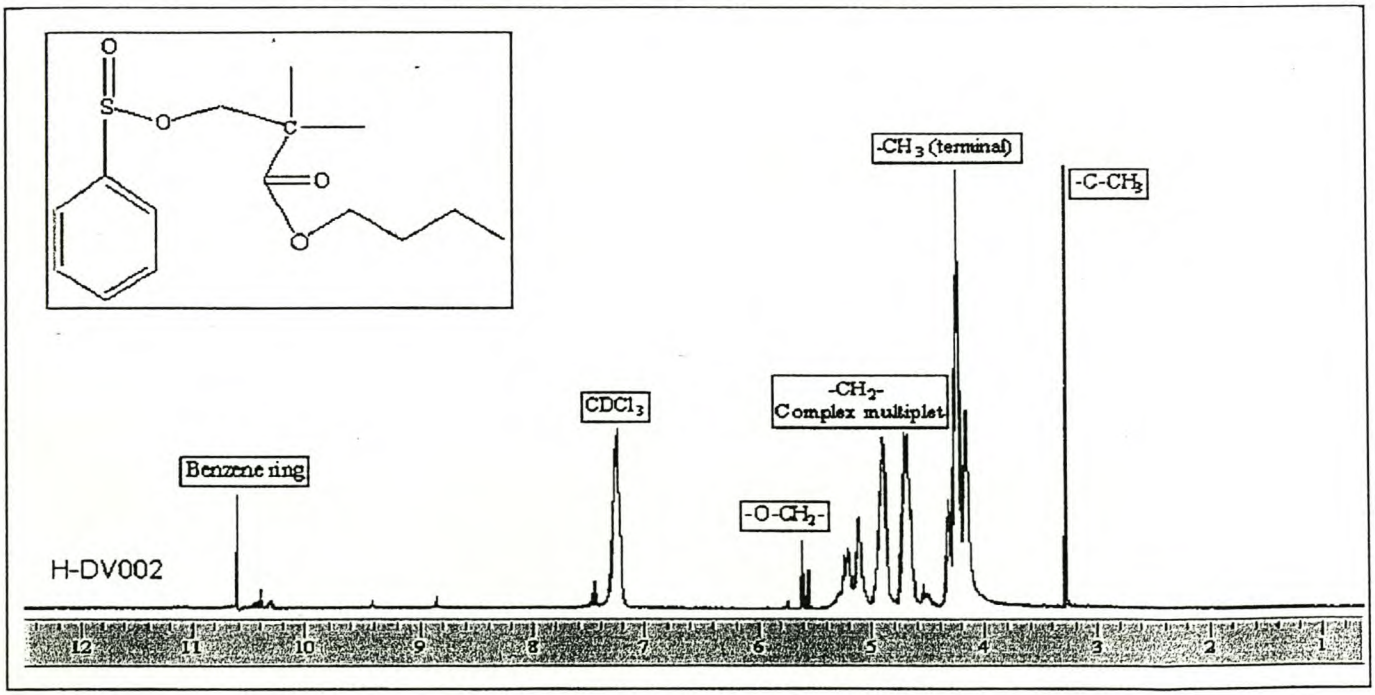

Node	Chemical shift [ppm]
Benzene ring	10.61
$CDCl_3$	7.25
-O-CH_2-	5.60
-CH_2-	4.92
-CH_3	4.25
-C-CH_3	3.30

E.2.2 Carbon-13 NMR of poly(n-butyl methacrylate)

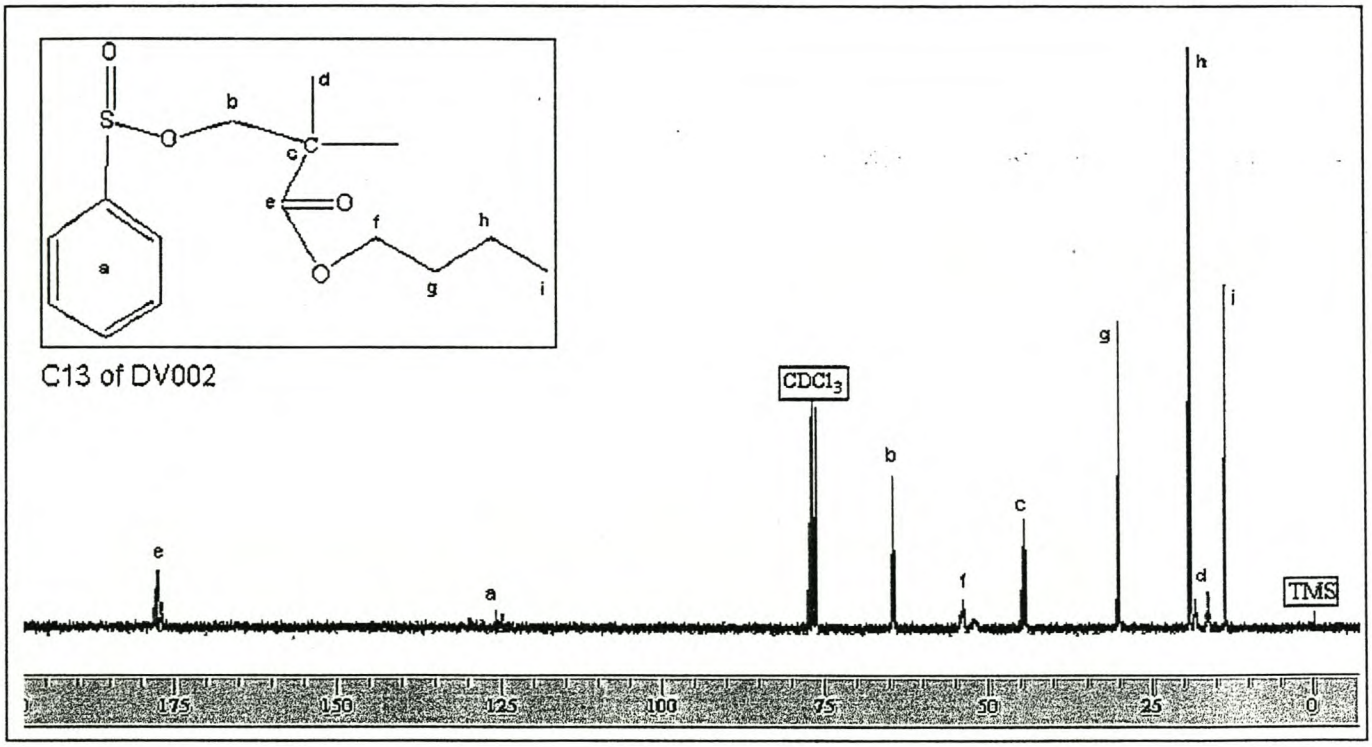

Node	Chemical shift [ppm]	Node	Chemical shift [ppm]
a	126.97	g	30.28
b	64.96	h	19.24
c	44.99	i	13.72
d	17.40	$CDCl_3$	76.99
e	177.67		
f	54.19		

E.2.3 Attached proton test (APT) of poly(n-butyl methacrylate)

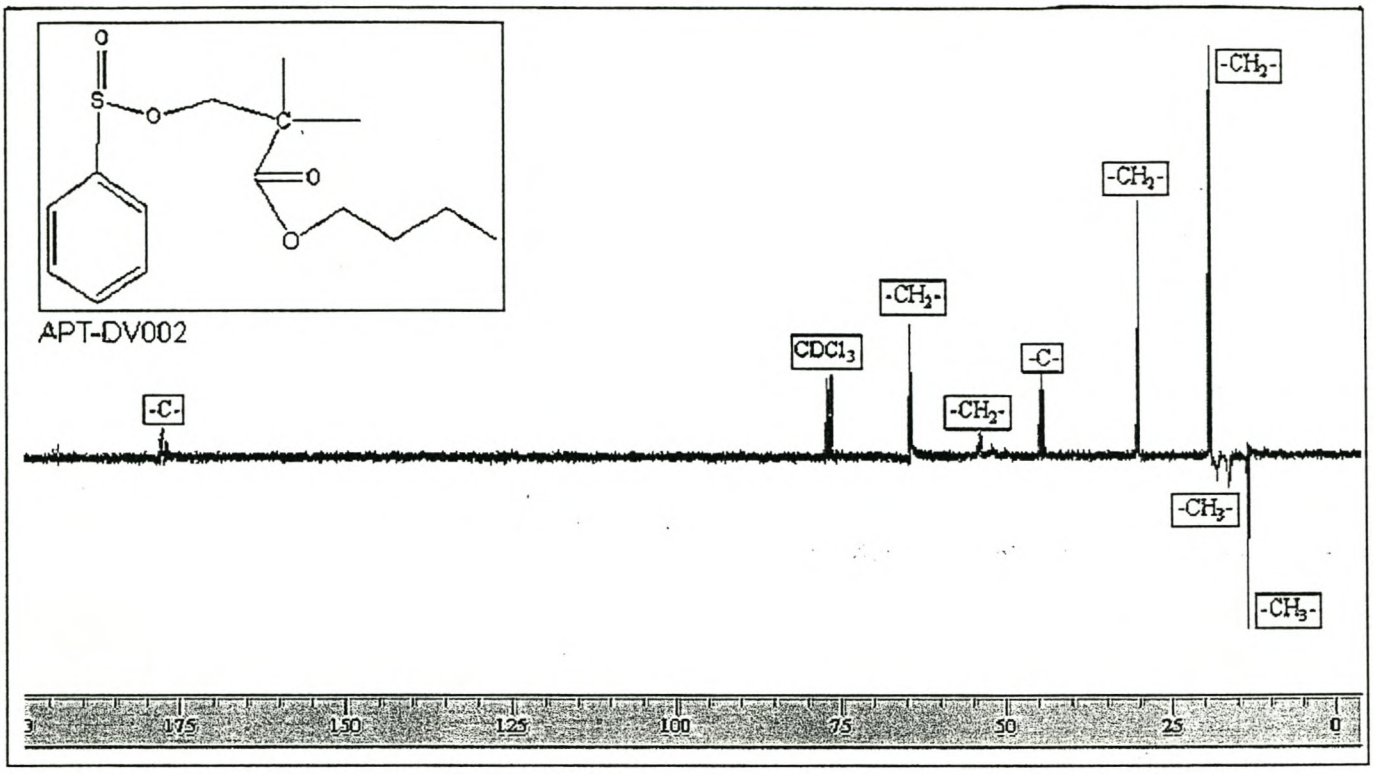

APPENDIX F

Comparison of the infra red spectra of poly(n-butyl methacrylate) where the Cu-PMDETA and the Cu-TMEDA complexes were used as the catalysts, respectively, in the polymerization process.

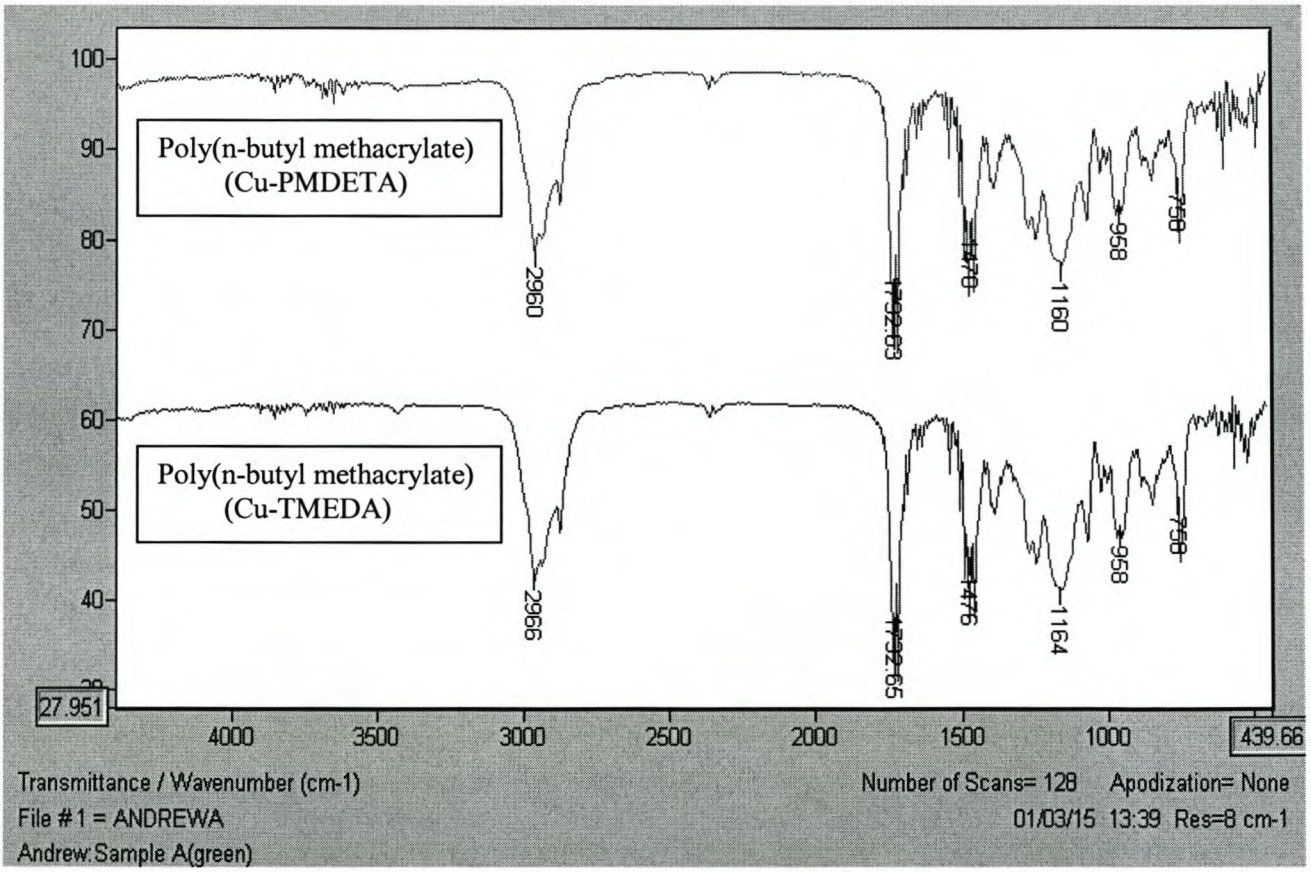

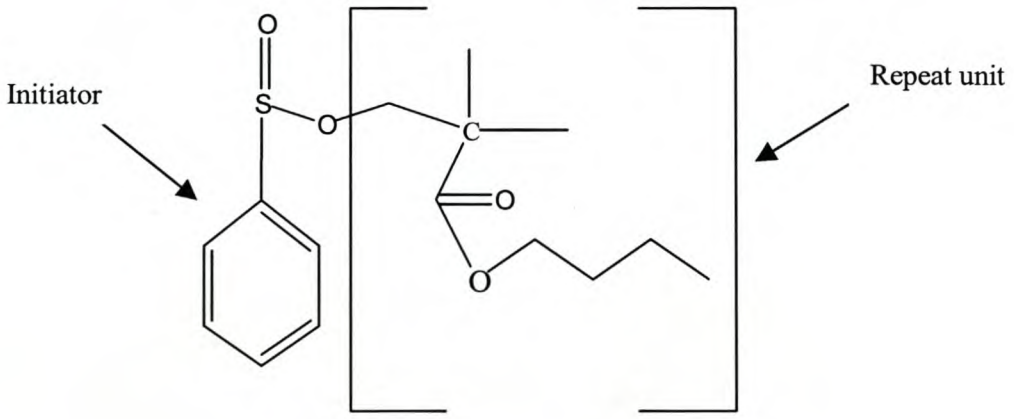

Node	Wavenumber [cm^{-1}]
ester	1732
sulphur	1156
benzene ring	1470-740
alkanes	2960, 1470, 750